Brno University of Technology
Faculty of Mechanical Engineering
Institute of Machine and Industrial Design

Vysoké učení technické v Brně
Fakulta strojního inženýrství
Ústav konstruování

Performance Evaluation of Products for Rail Head

Ing. Martin Valena
Author
Autor práce

prof. Ing. Martin Hartl, Ph.D.
Supervisor
Vedoucí práce

Dissertation thesis
Dizertační práce

Brno 2024

STATEMENT

I hereby declare that I have written the PhD thesis *Performance Evaluation of Products for Rail Head* on my own according to the advice of my supervisor prof. Ing. Martin Hartl, Ph.D., and using the sources listed in the references.

.....
Martin Valena

BIBLIOGRAPHICAL REFERENCE

VALENA, Martin. *Performance Evaluation of Products for Rail Head*. Brno, 2024. 135 p., PhD thesis. Brno University of Technology, Faculty of Mechanical Engineering, Institute of Machine and Industrial Design. Supervisor prof. Ing. Martin Hartl, Ph.D.

ACKNOWLEDGEMENT

I would like to express my gratitude to Prof. Ing. Martin Hartl, Ph.D., for his support during my studies. Special thanks go to Ing. Milan Omasta, Ph.D., for his help, support, and valuable discussions. My deepest appreciation goes to Ing. Radovan Galas, Ph.D., for his great efforts in assisting me with all aspects of my research.

I would also like to thank my colleagues at the Institute of Machine and Industrial Design. Special thanks to the colleagues/friends with whom I shared an office, where we had a pleasant, supportive, creative, and fun atmosphere. I must not forget to acknowledge my friends in firefighter sport, with whom I experienced tons of fun, which kept me uplifted and energized.

Finally, my most heartfelt thanks go to my family for their enormous support.

ABSTRACT

This dissertation deals with the design of a multi-phase methodology for evaluating the performance of top-of-rail products and the development of a portable rail tribometer. Based on the literature, the following performance parameters were identified: coefficient of traction, creep curve shape, retentivity and carry distance. Most of the studies performed measurements on different equipment and with different methodologies, which makes the results difficult to compare and indicates the need for a uniform methodology. The first phase of the methodology uses a universal tribometer, which allows for transferability and comparability of results across sites. This phase is used to identify the best-performing top-of-rail product based on the four performance classes. This product can be further tested under conditions closer to real operation, which represents the second phase of the methodology. In the second phase, track performance parameters are determined: retentivity, carry distance and risk of over-lubrication, and the effect of quantity and application strategy can be studied. To evaluate these parameters, a rail tribometer has been developed, capable of determining the coefficient of traction and the shape of the creep curve on the rail both in the laboratory and in the field. The tribometer is mounted to the rail and the measuring module performs a movement, varying the braking torque applied to the wheel and thus inducing a creep in contact. The third phase focuses on the investigation of the third-body layer in the field that is affected by weather conditions. Simultaneously, a noise module was used for monitoring noise parameters in a sharp curve. A significant correlation between the results of the first and second phases was found. Oil-based products provide longer retentivity and carry distance than water-based products, but are more prone to critically low friction. However, this drop does not reach critically low values on the actual rail as with universal tribometers and occurs only at the point of application. A further finding is a significant correlation between the traction coefficient and the duration of squeal noise, indicating that the duration of the noise is a suitable parameter for assessing howling noise.

KEYWORDS

Wheel-rail contact, portable rail tribometer, top-of-rail product, methodology evaluating performance, third-body layer

ABSTRAKT

Tato disertační práce se zabývá návrhem vícefázové metodiky pro hodnocení výkonnosti maziv na temeno kolejnice a vývojem přenosného traťového tribometru. Na základě literatury byly identifikovány následující výkonnostní parametry: součinitel trakce, tvar trakční křivky, retentivita a délka ošetření kolejnice. Většina studií prováděla měření na rozdílných zařízeních a s rozdílnou metodologií, což ztěžuje porovnatelnost výsledků a ukazuje na potřebu jednotné metodiky. První fáze metodiky využívá univerzální tribometr, který umožňuje její přenositelnost a porovnatelnost výsledků napříč pracovišti. Tato fáze slouží k identifikaci nejvýkonnějšího produktu pro temeno kolejnice na základě čtyř výkonnostních tříd. Tento produkt je pak možné dále testovat za podmínek bližších reálnému provozu, což představuje druhá fáze metodiky. Ve druhé fázi se stanovují reálné výkonnostní parametry: retentivita, délka ošetření kolejnice a riziko přemazání kontaktu a je možné studovat vliv množství a aplikační strategie. Pro vyhodnocení těchto parametrů byl vyvinut traťový tribometr, schopný stanovit součinitel trakce a tvar trakční křivky na kolejnici jak v laboratoři, tak na trati. Tribometr se připevňuje ke kolejnici a měřicí modul vykonává pohyb, přičemž mění brzdný moment působící na kolo a tím vyvozuje skluz v kontaktu. Třetí fáze se zaměřuje na výzkum třecí vrstvy v reálném prostředí, která je ovlivněna povětrnostními podmínkami. Současně byl použit hlukový modul pro monitorování hlukových parametrů v oblouku s malým poloměrem. Byla zjištěna značná korelace mezi výsledky první a druhé fáze. Ukázalo se, že olejové produkty poskytují větší retentivitu a délku ošetření kolejnice než vodní produkty, ale jsou více náchylné ke kriticky nízkému tření. Tento pokles však nedosahuje kriticky nízkých hodnot na reálné kolejnici, jak je tomu u univerzálních tribometrů, a vyskytuje se pouze v místě aplikace. Dalším zjištěním je, že existuje významná korelace mezi součinitelem trakce a dobou trvání kvílivého hluku, přičemž délka hluku se jeví jako vhodný parametr pro hodnocení kvílivého hluku.

KLÍČOVÁ SLOVA

Kontakt kolo-kolejnice, přenosný traťový tribometr, mazivo na temeno kolejnice, metodika na hodnocení výkonnosti, třecí vrstva

CONTENT

1 INTRODUCTION

Rail transport is essential for freight and passenger transport due to its low energy consumption and reliability. Increasing efficiency and economy in transport has become crucial, and one key area of focus is the control of friction between the wheel and rail to maintain an optimal coefficient of friction (CoF). A high CoF leads to excessive wear on rail wheels and rails, resulting in shorter service intervals and higher maintenance costs. Conversely, very low friction can cause traction issues and increase safety risks due to longer braking distances. The costs associated with low adhesion are estimated at 90 million euros across Europe. While sanding is a common solution for poor adhesion, it can cause additional wear and, in critical cases, loss of conductivity affecting vehicle localisation.

Different requirements are imposed on substances applied to the top of the rail and the gauge corner, referred to as top-of-rail products and lubricants, respectively. The railhead, where traction and braking forces are transmitted, requires an intermediate level of friction and a positive creep curve. This leads to reductions in fuel consumption, corrugation, wear, and noise. In contrast, the gauge corner, which comes into contact with the wheel flange, requires minimised friction to reduce wear, noise, and the risk of derailment.

These products are tested on various devices with different scales and levels of simplification in both the laboratory and the field. Each testing variant is suitable for determining different product parameters including CoF, creep curve trend, retentivity, and carry distance. Other consequential parameters include noise reduction, wear, and rolling contact fatigue (RCF). Field tests provide the most relevant results but are less repeatable and transferable due to external influences such as weather conditions, contaminants, and real friction layers with oxides and wear particles. Additionally, field tests are time-consuming and expensive. Conversely, laboratory tests are cheaper, less time-consuming, and provide well-controlled conditions, but often involve a significant degree of simplification. Using samples made from actual materials or full-scale facilities can reduce the simplification. Another approach is to use portable tribometers that allow measurements in both the laboratory and the field. Comparing results using the same methodology in both settings provides a better understanding of real friction layer formation.

The aim of this thesis is to develop a methodology for evaluating the performance of top-of-rail products at several levels of simplification. The methodology will provide comparative tests that can be carried out across different laboratories. They aim to identify the best-performing product, which may be further tested under configuration closer to actual wheel-rail contact. Significant effort will be dedicated to developing a portable tribometer that can be used both in the laboratory and in the field and will help assess track performance parameters.

2 STATE OF THE ART

2.1 Wheel-Rail Interface

The wheel-rail interface is an open tribological system, so the frictional properties are affected by weather conditions and many substances from which some occur naturally whereas others are added artificially. Typical representatives of natural contaminants are water, dust, oxides, and leaves. Artificial substances aim to provide desired friction conditions in the contact. They are further divided according to their purpose in the chap. 2.2.

The contact between the wheel and the rail occurs in two places, see Fig. 1. The first is between the wheel tread and the top of the rail, where traction and braking forces are transferred, allowing the train to start and stop. This contact also transmits the normal forces corresponding to the weight of the car. In contrast, contact between the wheel flange and the rail gauge corner occurs only when the train negotiates a curve. This contact transmits large forces and experiences considerable slippage. Wear occurs in both contacts, although through different mechanisms. One way to reduce this wear is through friction management.

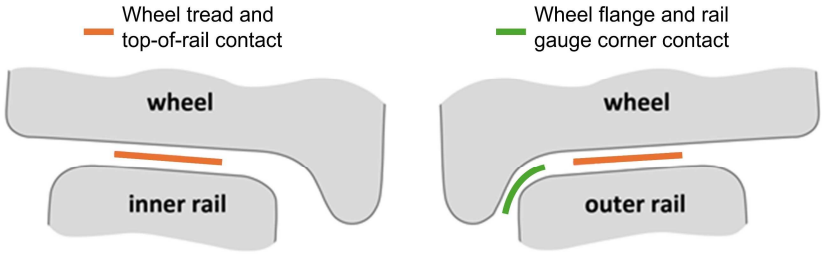

Fig. 1 Contacts in the wheel-rail interface

2.1.1 Key Terms for Wheel-Rail Interface

The most important is the CoF characterising frictional properties and is defined as a ratio between the tangential frictional force F_F and normal force F_N in contact between two surfaces, see Eq. (1). This is defined for pure sliding conditions, but the wheel performs a combination of translation and rotational movement, while the torque is applied to it. The wheel-rail contact transfers lateral, and longitudinal forces beside normal force. The longitudinal forces (also referred to as tangential, traction or creep forces) act during acceleration or braking, while lateral forces are perpendicular to the direction of motion and hold the vehicle on the rails. Their magnitude may reach up to the limiting friction force defined by CoF. These forces are also referred to as adhesion forces, thus a coefficient of adhesion (CoA) or traction (CoT) may be defined similarly to CoF, see eq. (2).

$$f = \frac{F_F}{F_N} \tag{1}$$

$$\mu = \frac{F_T}{F_N} \leq f \tag{2}$$

As the wheel-rail contact transfer torque, it does not operate under pure rolling conditions, which makes the understanding of the contact difficult. It operates under rolling-sliding conditions meaning that a part of the contact adheres together (also called a stick area) while the other part of the contact is under micro-slip. If the contact does not transmit any tangential force, i.e. there is pure rolling, only the stick area appears in the contact. When the transmitted force is increased, microscopic slip occurs, resulting in the formation of a slip area and a reduction in the stick area in the contact. When the force is equal to the frictional force defined by the CoF, the entire contact is in micro slip mode. This occurs at around 1-2% slip. This theory was first described mathematically by Carter [1] in the early 20th century. The experimental confirmation of this theory came in the 1960s with the use of photoelasticity by Haines and Ollerton [2].

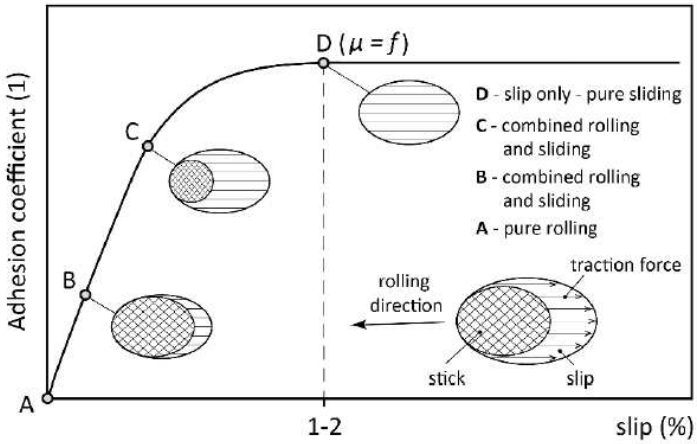

Fig. 2 Theoretical creep curve according to Carter [3]

The other important parameter characterising the contact is slip, also referred to as a creep, which is connected with the relative speed between the surfaces. The slip-to-roll ratio (SRR) is usually used in a laboratory due to the kinematics of devices, see eq. (3), while slip is used in terms of running vehicle, see eq. (4).

$$SRR = \frac{2(v_1 - v_2)}{v_1 + v_2} \tag{3}$$

$$slip = \frac{v_1 - \omega_1 r}{v_1} \tag{4}$$

2.1.2 Problems in Wheel-Rail Contact

The interaction between railway wheels and rails presents several challenges that can affect the performance and longevity of railway systems. Key issues include wear, corrugation, and noise, which significantly impact the efficiency, safety, and comfort of rail operations. These issues are primarily related to the operational conditions at the contact point and the inherent complexity of the system.

Wear is the loss or displacement of material from a contacting surface [4]. A material can be worn by several different mechanisms or modes. How a material wears depends on the nature of the material, weather conditions, presence of contaminants and operating parameters. Wear is mainly related to high contact pressure and sliding motion in the tangential direction, which is more severe than motion perpendicular to the surface, such as an impact. This process generates a noticeable amount of heat that can lead to thermal softening or even thermal breakdown. Wear is characterized by the wear rate, which is the volume of material lost per unit of distance travelled or per unit of time.

A typical problem on the track is corrugation. In the railway field, six types of corrugations are distinguished, varying in wavelength, damage mechanisms, and locations [4,5]. Corrugation, particularly short-pitch corrugation, is characterized by a uniform wavelength with an amplitude of tenths of a millimetre and a frequency between 250–400 Hz. This type typically occurs on the low rail of curves due to roll-slip oscillation. It is initiated by wheel-rail surface irregularities and the trend of the traction curve. Contributing factors include poor alignment of wheelsets and the close conformity between wheel tread and rail. These conditions lead to patches forming on contact surfaces, which grow into corrugation valleys, causing increased noise, wheel squeal, and wear.

Besides the rolling noise arising from irregularities and roughness of the wheel and rail and impact noise caused by rail connections and flats on the wheel thread, the squeal noise appears in sharp curves with a radius of 200 m or less [6] and it is very annoying because it is louder than rolling noise. The curve squeal can be further categorized into squeal noise and flange noise, both of which are associated with frictional instabilities at the contact points [7]. Flange noise arises when the wheel flange contacts the gauge face of the rail [6], typically involving the outer leading wheel or inner trailing wheel. This type of noise is characterized by a wide frequency range of 5-10 kHz [8]. On the other hand, lateral slip or creep between the wheel tread and the top of the rail significantly contributes to the generation of squeal noise, also referred to as top-of-rail squeal. This noise has a pronounced tonal quality and usually falls within the 400 Hz to 5 kHz range [9]. Additionally, longitudinal creep influences squeal noise, which occurs within the 3.5-6 kHz frequency band [10]. Both squeal and flange noises are affected by various factors, including operating conditions, rolling speed, angle of attack, track geometry, and dynamics, making them highly unpredictable and only estimable with some degree of probability [11–13]. The noise is

generally characterized by sound power level [14] or sound pressure level (SPL) [15]. Other parameters characterising the noise occurrence were introduced, like an occurrence frequency [14] and probability of squeal [12]. As the curve squeal is closely related to the wheel and rail vibration, the natural frequencies, mode shapes and damping ratio of the bodies are important [16,17].

2.2 Friction Management

As mentioned above, the contact between the wheel and the rail occurs in two areas, each operating under different conditions with distinct frictional requirements. The goal of friction management for wheel flange-rail gauge corner contact is to minimise wear by achieving a very low CoF. This also reduces unwanted tangential forces. For the wheel tread-top of rail contact, the objective is similar—to minimise wear and corrugation by lowering the CoF. However, unlike the wheel flange contact, reducing the CoF to a minimum is not feasible, as this would compromise the transmission of traction and braking forces. Therefore, the aim is to lower the CoF to a level that ensures safe operation while still providing the necessary traction and braking performance.

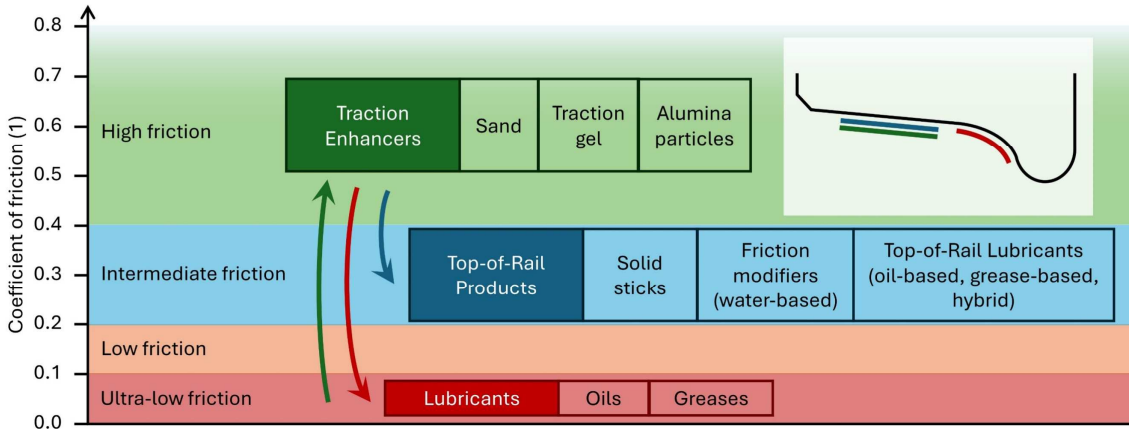

Fig. 3 Wheel/rail friction regimes and actions required by friction management products

The division of products applied into the wheel-rail interface is carried out according to the articles [18,19], see Fig. 3. The first group is a low coefficient of friction modifiers (called lubricants), such as grease and oil, that are applied on the flange or the gauge rail and decrease the CoF and wear. The traction enhancers (also referred to as very high positive friction modifiers – VHPF) are applied on the top of the rail when poor traction conditions occur. The most common representative is sand which is reliable but significantly damages the bodies and pollutes the rail track surroundings. In case of dry conditions, the CoT is considered too high and it is desired to decrease and maintain it at a desired level. For this purpose, top-of-rail (TOR) products (also referred to as high positive friction modifiers) were developed. The other required property of TOR products (TORP) is a positive friction characteristic, which means that the CoT increases with increasing creep.

The TORP can be further divided according to their base medium ensuring their transferability. Water-based substances are called friction modifiers (FM) and are meant to dry out after the substance is spread along the rail. After drying, the FM creates a third body layer that can absorb a portion of shear deformation in the contact. The oil-based and grease-based products do not dry and are called TOR lubricants (TORL). Products that contain both water and oil are referred to as TOR hybrid, but they are often classified as TORLs. These substances reduce the CoT because they provide a boundary and mixed lubrication regime. The abovementioned TORPs are more or less liquid, but solid materials were also developed in the form of interlocking sticks called solid sticks [20]. Fig. 3 shows the friction regime and the changes in the CoT due to friction management.

The TORPs have many benefits which come from the intermediate level of CoT and positive friction characteristics. The lower CoT leads to a reduction of lateral forces [18,21,22] especially in sharp curves, which subsequently improve curving performance and decrease in risk of derailment [23,24]. It also results in lower longitudinal forces acting on the rear wheelset. As a result, the moment displacing the outer front wheel to the flange contact position is reduced, thus reducing the flange contact force. Another benefit arises also from the intermediate CoT and is lower energy consumption [22,25]. The application of TORP can reduce wear and RCF [19,26,27]. A study [27] showed that both benefits may be achieved at once. On the other hand, paper [19] discussed that these mechanisms are slightly contradictory because a higher wear rate can stop the crack growth or even reduce its length. The reduction of corrugation [28–30] and noise [8,15,31] is connected with positive friction characteristics because it prevents stick-slip oscillations. In the case of noise, the oscillations vibrate the wheel which further emits these vibrations in the form of squeal noise.

TORPs have not only benefits but also have some downsides. The major one is that the abovementioned advantage can be achieved only when an appropriate amount is used. Otherwise, over-lubrication may occur, which causes a very low CoT compromising traction and prolonging braking distance. This was observed for TORL [32] and also for FM [33]. Moreover, TORPs are usually studied under clean conditions and any contamination is neglected. Iron oxides can alter the resulting CoT in a positive way when they are mixed with FM [34]. On the other hand, water acts in the opposite way, a very low CoT may occur when TORL is contaminated by water [35]. In the case of FM, a small amount of water can extend the lasting effect, however, an excessive amount flushes the FM out resulting in shorter performance. Abbasi [36] observed that TORPs generally reduce the amount of air-borne particles while TORLs are significantly more effective, but FM generate multiple times more ultrafine particles than was observed for dry contact.

The research of TORP behaviour is carried out in both field and laboratory. The field measurements [29,31,33] are the most representative and provide reliable results. On the other hand, they are very expensive, time time-consuming, and the conditions in the wheel-rail contact are not well-controlled, as they are affected by many circumstances like weather

conditions, dust, oxides and so on. In contrast, laboratory experiments are performed under well-controlled conditions and are significantly cheaper and less time-consuming, but some simplifications are introduced. There are many devices with different scale factors. Pin-on-disc tribometer [36–38] operates under pure sliding conditions, which do not represent actual contact well and it is commonly used for wear tests. A device with more representative contact is a ball-on-disk tribometer [35,39–41] operating under rolling-sliding contact. Both specimens are usually driven separately, so exact SRR values can be maintained during an experiment. Twin-disc machines [32,42–44] are closer to the actual wheel-rail contact because specimens can be cut directly from the wheel or rail or are made of similar steel. The discs create a point or line contact depending on the disc geometry and work under rolling-sliding conditions. These devices are used for almost all types of experiments. Devices in similar configurations were developed. For instance, discs were replaced with rollers [24], one disc was exchanged for a cylinder [45], or even a scaled wheelset was used [46]. Full-scaled facilities are the closest to reality because they use actual wheel and rail [47], or the wheel and scaled disk representing the rail [12,48,49], which is more common, but facilities with larger rail discs also exist [23,50,51]. Each of the mentioned facilities has a unique construction and is highly customized. Somewhere between field and laboratory, rail tribometers are located. These devices allow us to measure the CoT on the rail no matter where the rail is. Several types were developed which are described further.

2.2.1 Third-Body Layer and Effect of the Weather Conditions

The term "third-body layer" refers to substances in the wheel-rail contact that fully or partially separate the surfaces, depending on the layer thickness. This layer forms naturally on the wheel and rail and consists of wear debris, oxide particles, contaminants, lubricants, and other materials. The third body layer is influenced by weather conditions, as the wheel-rail contact is an open tribological system, leading to varying tribological properties.

A study [52] investigated the formation of iron oxides on the railhead surface in moist and salty environments. In a moist environment, γ-FeOOH, α-FeOOH (red rust), and magnetite (Fe_3O_4) formed, with concentrations varying across the railhead, but magnetite was mainly present on the gauge corner. The salty environment additionally generated β-FeOOH. The study also showed that different pre-conditioning procedures, such as grinding with abrasive paper and degreasing, affected the composition of the resulting oxides, each influencing the CoT differently [53].

In studies [54] and [55], a pin-on-disc tribometer with a climate chamber was used to set various temperatures and relative humidity (RH), leading to the formation of different oxides on contact surfaces. Three iron oxides found at the wheel-rail interface were identified: wustite (FeO), magnetite, and hematite (Fe_2O_3). Hematite, along with humidity, influences the friction curve shape, while magnetite forms in damp environments and protects against

severe wear. Results showed hematite significantly affects the friction coefficient under boundary lubrication, preventing a significant reduction in friction by water vapour. Additionally, the friction coefficient decreases with increasing RH, especially at low RH levels, see Fig. 4.

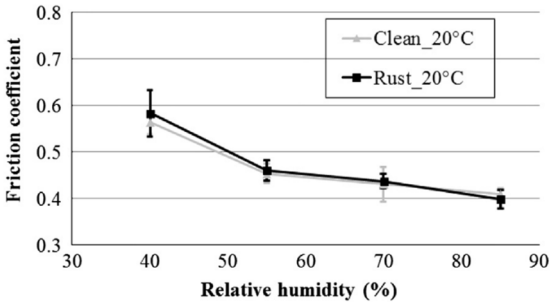

Fig. 4 Effect of RH on the CoF [55]

A similar observation was performed in the study [56] where the effect of RH and temperature was investigated under rolling-sliding contact with clean and leaf-contaminated discs. Tests were conducted at various constant temperatures. It was shown that increasing RH reduces the CoA under all tested conditions, with a nearly linear trend (Fig. 5), contrasting with the findings in the study [55]. When the temperature is above 30 °C, the decrease in CoA is nearly negligible, whereas below 24 °C, the effect becomes substantial. Low temperature and high RH led to condensation, resulting in a significant drop in CoA, especially for contaminated discs, where CoA reached as low as 0.05.

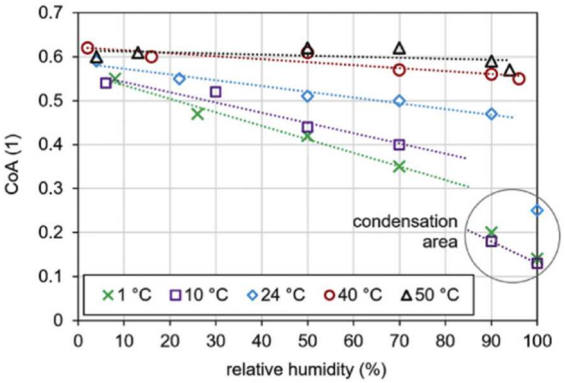

Fig. 5 Effect of RH and temperature on CoA for clean disc [56]

2.3 Experiments in Laboratory

2.3.1 Effect of TOR Products on CoT

The performance of TORP in laboratory settings has been the subject of research since 2002. Matsumoto et al. [46] first investigated this using a scaled roller stand (1/5 scale) to observe how a liquid FM affects the shape of longitudinal and lateral creep curves. Their findings

demonstrated that the liquid FM could counteract the negative trends in these curves typically seen under dry conditions, see Fig. 6. However, this study did not address the impact of FM on CoT, but it is obvious from figures that CoT was reduced from 0.45 to 0.17 and the gradient of initial creep curve part is lower.

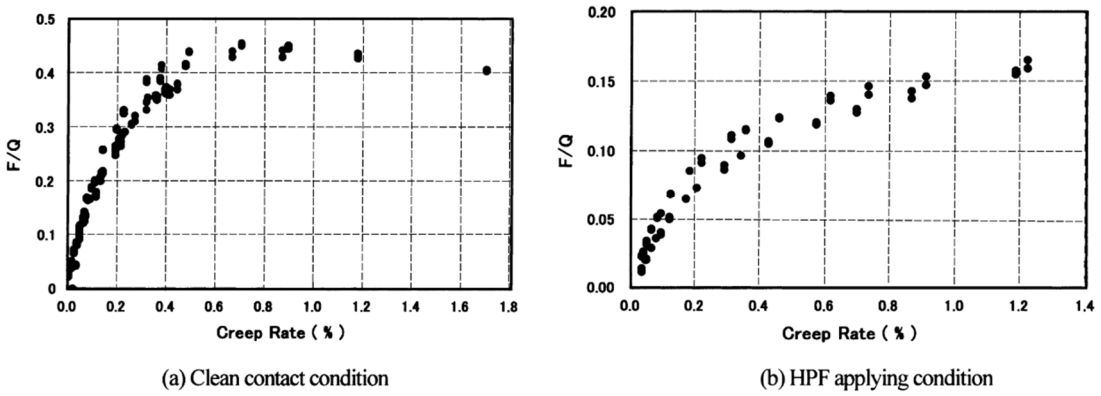

Fig. 6 Longitudinal creep force characteristic: a) clean contact condition; b) HPF applying condition [46]

Following this, the same researchers utilised a 1/10-scale model vehicle to explore the effects of FM on adhesion through multiple passes in a tight curve with a radius of 3.3 meters [24]. In this experiment, Keltrack™ FM was applied to the top of the low rail using a nozzle. As depicted in Fig. 7a, the adhesion coefficient significantly dropped to around 0.15 immediately after application (noted in the 21st test), followed by a gradual return to the dry CoT level. This pattern is repeated after each FM re-application. Further experiments were performed with a twin-disc machine to achieve an optimal balance between FM supply and consumption. These tests varied the spraying duration (0.2, 0.4, and 1.0 seconds), slip values (0–2%) and time between applications. Authors observed that an amount of FM can alter the creep curve shape, while 0.2 s of spraying duration results in a higher gradient. Higher amounts of FM also led to lower CoT, but the effect of 1 s and 0.4 s is the same. The slip in the contact affects the consumption of FM, see Fig. 7b. When the slip was doubled the time before reaching the maximum value was approximately halved, simultaneously the max. value was lower for lower slips. In addition, the shorter intervals between applications caused the FM not to be completely consumed and therefore the CoT decreased in subsequent tests. In the case of 80-second intervals between applications, no trend was observed on subsequent tests.

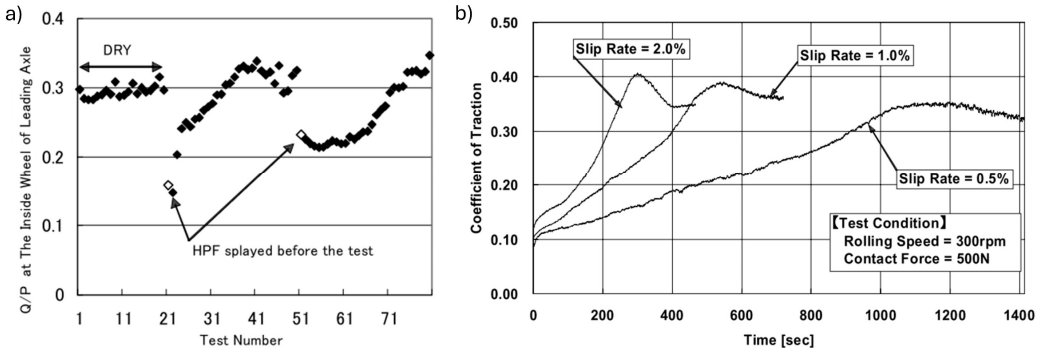

Fig. 7 a) Effect of vehicle passes on CoT, b) the effect of slip rate on FM duration [24]

Tomeoka et al. [57] investigated the effect of FM and application methods on the creep curve. The discs were grounded by sandpaper and then rotated with a creep until the CoT was stabilised. After the application of FM via roller, several test cycles were performed. The first one provided CoT slightly above 0.1 (Fig. 8a), which is not substantial for braking without skidding. Subsequent cycles shifted the creep curves to higher CoT values, with intermediate values observed from the second to the seventh cycle, and after the ninth cycle, values like those for dry conditions were achieved. To address the issue of low adhesion after application, the authors proposed using a spraying mist to distribute the product more evenly. Fig. 8b shows the resulting creep curves, which provided intermediate CoT from the second to the fourth cycle. The authors developed an on-board unit and tested it in operation. It led to a reduction of tangential forces up to 70% and noise level by 20 dB.

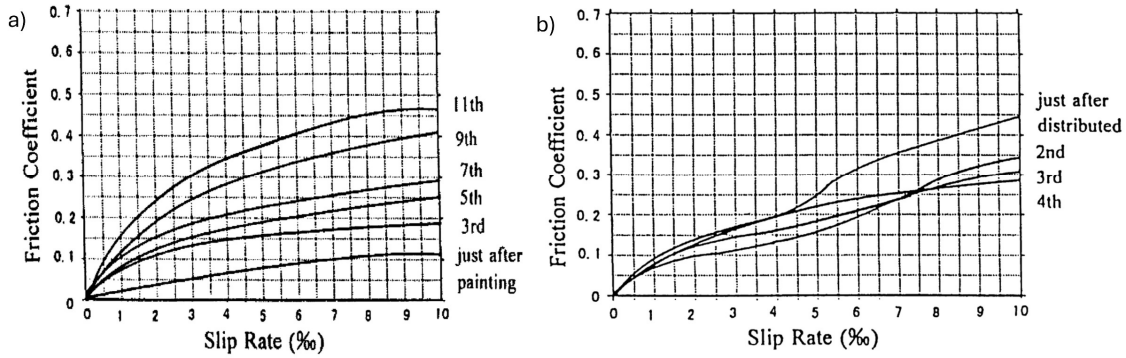

Fig. 8 Creep curves for a) painted FM and b) sprayed FM [57]

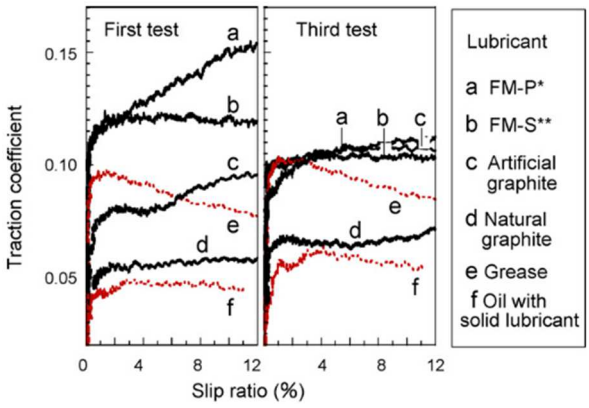

Fig. 9 Traction characteristics of lubricants [58]

Ishida et al. [58] used the twin-disk machine to evaluate the performance of developed FM and other lubricants. The specimens were made of actual materials and polished #80 sandpaper before the test followed by a 5 min run-in (in the text refer as warm-up), which resulted in R_q of about 1 µm. The circumferential speed was 40 km/h and Hertzian pressure was 670 MPa. The developed FMs reported the highest CoT and FM-P had a positive slope while FM-S had a negative one in the first test, see Fig. 9. Both overperformed the rest of the tested products whereby product "f" was an FM for a top of low rail and was getting popular. In the third test, the CoT was lower than that in the first test, simultaneously the slope for FM-P was smaller.

Studies [42,59] investigated the effect of a solid stick friction modifier on rail insolation and the CoT. The authors employed a twin-disc machine with discs cut from the R8T wheel rim and BS11 rail sections. The solid stick was pressed to the wheel disc by a spring. The first study was carried out under the contact pressure of 900 MPa with, a rotation speed of 400 rpm (1 m/s) and before the application of a solid stick, the run-in under dry conditions was performed until the stable CoT value was observed. The second study [59] used a contact pressure of 470 MPa and tangential speeds of 1 m/s and 0.3 m/s. In this case, the CoT and impedance were measured for 3000 cycles under dry conditions followed by another 3000 cycles with a solid stick. The slip varied from 0.1% to 3%. The authors showed that the impedance did not increase significantly and stayed below the maximum value obtained under dry conditions. In contrast, the CoT decreased from 0.6 and 0.4 to 0.28 and 0.24 for slips of 3% and 1%, respectively. The CoT gradually declined after the application of a solid stick and started rising after the end of the application (Fig. 10a), which was caused by the removal mechanism breaking down the created layer. The lower CoT was observed under a lower rolling speed. Moreover, the solid stick had a limited effect under low slips, it did not alter the CoT, see Fig. 10b.

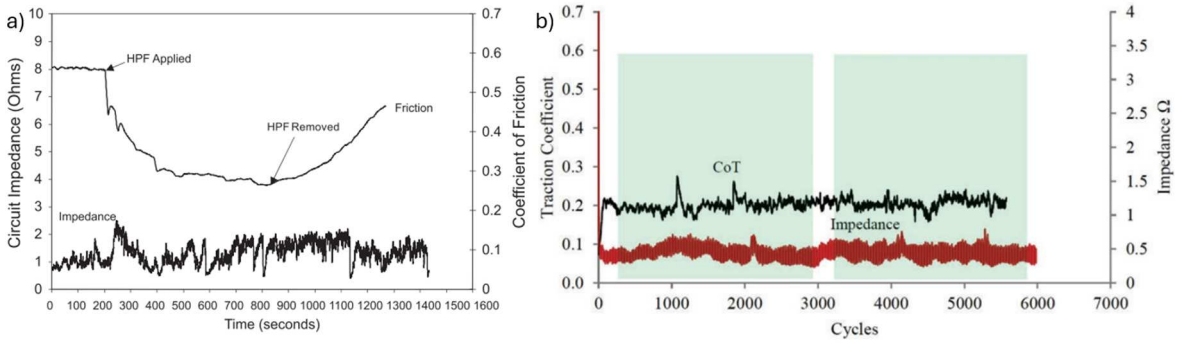

Fig. 10 The effect of solid stick on CoT and impedance under a) 3% of slip [42] and b) 0.3% of slip [59]

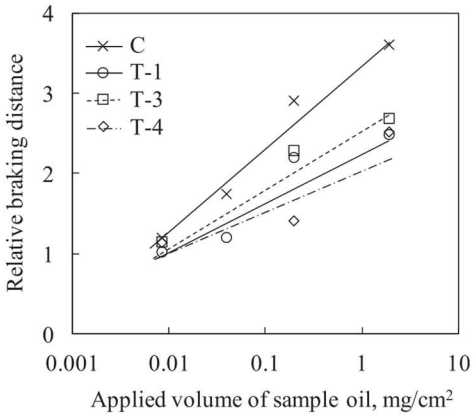

Fig. 11 Brake performance tests [60]

The CoT directly affected the braking distance which is crucial for safety. Sone et al. [60] studied the impact of traction fluid and the amount on braking distance. They utilized a full-scale rig and traction fluid was applied via a micro syringe. After the fluid application, the wheels rotated to enter the fluid into the contact area. When the circumferential speed

reached 130 km/s a DC motor was disconnected, and the wheel was braked. The test ended when the speed reached 90 km/s. Fluids were applied in three dosages used on the actual track and one excessive amount. The authors observed that traction fluids prevented sliding during tests; thus, the control system should not adjust the braking power. Fig. 11 shows the effect of traction fluid (referred to as T) on relative braking distance which is normalized to that obtained without lubrication. The braking distance is prolonged with higher amounts of fluids and traction fluid reached half of that observed for a conventional oil lubricant. The authors also identified that the scatter of braking distances was caused by varying roughness. When roughness is significant, the braking distance is shorter because the oil film in the contact is broken by the asperity of surface roughness.

The pin-on-disc tribometer with a climate chamber was utilized to study the effects of iron oxides, humidity and temperature on the performance of FM [34]. The contact pressure of 900 MPa was induced by dead weight and a sliding speed of 0.01 m/s was used. The mixture of FM and oxides was applied directly to the pin. The experiment was carried out with pure FM and a mixture of FM with several oxide concentrations, while temperature and RH also varied. The tests lasted for 30 minutes to allow the drying of substances. The study provided much information about the behaviour of FM under contamination and weather conditions. Authors observed that black and red oxides increase CoF over the that recorded for pure FM. The CoF was low (around 0.3) during the whole test when the RH was high (above 70%) while the CoF rose under 40% of RH, see Fig. 12. It indicated a retardment of water evaporation and maintained the substance wet. When the drying process started the CoF increased to that observed for dry conditions. The effect of temperature relates to the concentration of oxides. The CoF rose under lower temperatures at a concentration of 25% whereas no change was observed for a concentration of 40%. The authors further specified that the transition point to the concentration range of 37% and 40%.

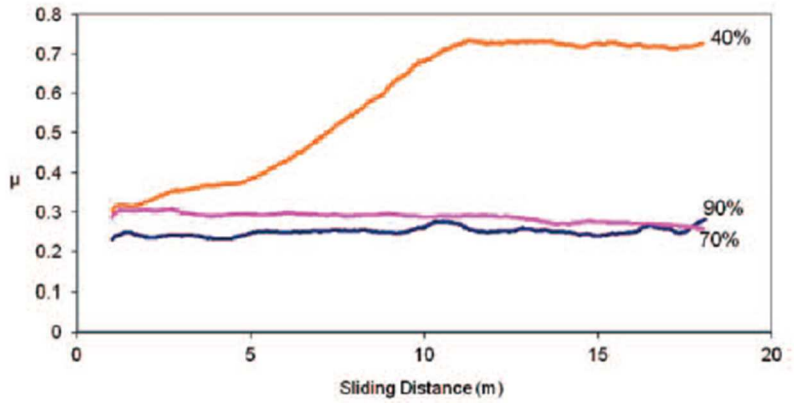

Fig. 12 The effect of RH on CoF for a mixture with 35% of black oxide [34]

Hardwick et al. [61] investigated the effect of water, gauge face lubricant, and several TORPs on RCF and recorded CoT during whole experiments. The authors used a twin-disc machine as in many abovementioned publications. The specimens were cut from the actual R8T wheel and R350HT rail with improved RCF resistance. A velocity of 1 m/s was

selected, with a contact pressure of 1500 MPa and a slip of 1%. TORPs were applied by a small brush or cotton swab at a rate of 0.05 g / 500 cycles, water dripped into the contact at a rate of 1 drip per second. Whole experiments lasted for 25000 cycles with the first 4000 performed under dry conditions to initialize RCF. The authors observed that the wear rate was reduced by FM, lubricant, and TORL (grease and hybrid), whereas it was significantly increased by water and oil TORL. In addition, all substances significantly reduced CoT, with water only reducing to 0.2, the rest below 0.1, and hybrid TORL reaching as low as 0.02. The FM and hybrid TORL exhibited a similar CoT pattern, as shown in Fig. 13, which related to the presence of water. In the case of FM, the differences in CoT before and after the application or reapplication are greater. Moreover, the CoT gradually decreased, which may indicate an inappropriate amount causing over lubrication.

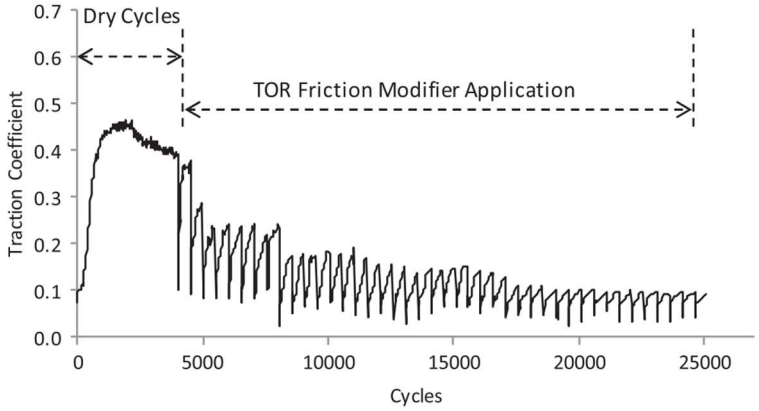

Fig. 13 Time evolution of CoT for FM [61]

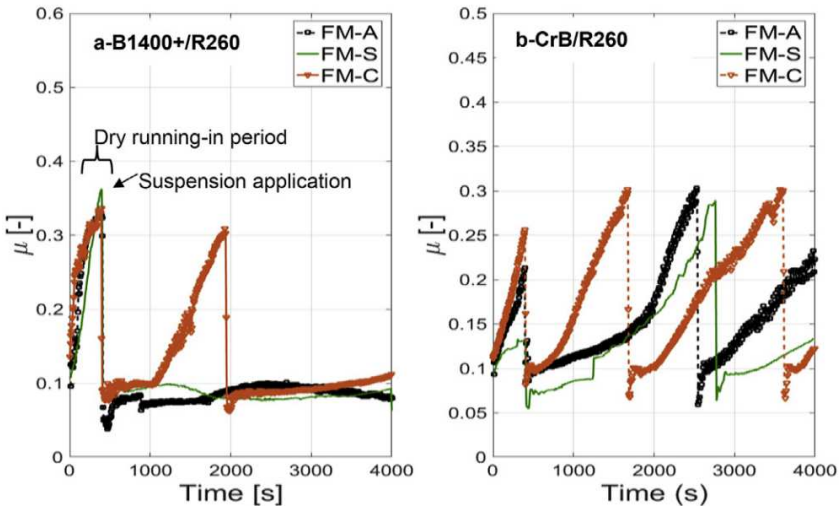

Fig. 14 Time evolution of CoT under 0.5% slip for three TORLs. a) B1400+ steel and b) CrB steel [62]

Messaadi et al. [62] investigated the frictional properties of newly developed rail steels with the presence of three oil-based TORLs. The horizontal twin-disc rig was employed to perform experiments under the contact pressure of 0.5 GPa and slip of 0.5% and 11%. Whenever the CoT reached 0.3, 20 µl of TORL was applied to the contact. Fig. 14 shows the significantly different behaviour of TORLs depending on the steel type and also the

difference between the TORLs. FM-C contained considerably larger and more prolonged copper particles compared to other samples. The copper particles were located on the edges of the contact band and caused a faster increase in CoT. The higher slip increased the number of applications during the experiments, which means that the consumption is higher. The authors showed that metallic particles adhered to the surface and created the 3rd body layer in different thicknesses depending on the steel. The particles can be entrapped in surface roughness.

Galas et al. [39] investigated the ability of TORLs to maintain intermediate CoT and reduce wear. The Mini Traction Machine (MTM) was employed with a ball made of AISI 1010 and a disc made of C45, similar to wheel steel R7T. The conditions were as follows: contact pressure 750 MPa, SRR 1-10% and speed 300 mm/s. The specimens were ultrasonically cleaned before the tests followed by a run-in under dry conditions and SRR according to the friction test. The run-in was stopped once the CoT was stabilised. Two commercial TORLs (labelled as FMA and FMB) were examined at several dosages, applied with a micropipette and further redistributed over several cycles. The main test lasted for 540 cycles. Laser particle analysis showed that FMA contains 40 times more solid particles larger than 4 µm than FMB. Both TORLs strongly depended on the applied amount (Fig. 15), but FMB is more sensitive, likely due to its smaller amount of particles. An application of 1 µl provided intermediate CoT (0.2-0.4) for only a few cycles with FMA and around 40 cycles with FMB. A larger amount extended this duration to hundreds of cycles, though FMA maintained a higher CoT. However, 4 µl of each TORL did not reach the lower limit. Immediately after application, the CoT dropped to 0.1, indicating over-lubrication, which means insufficient CoT for braking and traction. FMA can recover from this drop faster and spends less time below a CoT of 0.15, reducing the risk of over-lubrication. Additionally, Stribeck curves were measured for both TORLs and castor oil under fully flooded conditions. The results show that both TORLs behave very similarly to castor oil in the transition from mixed lubrication to elastohydrodynamic.

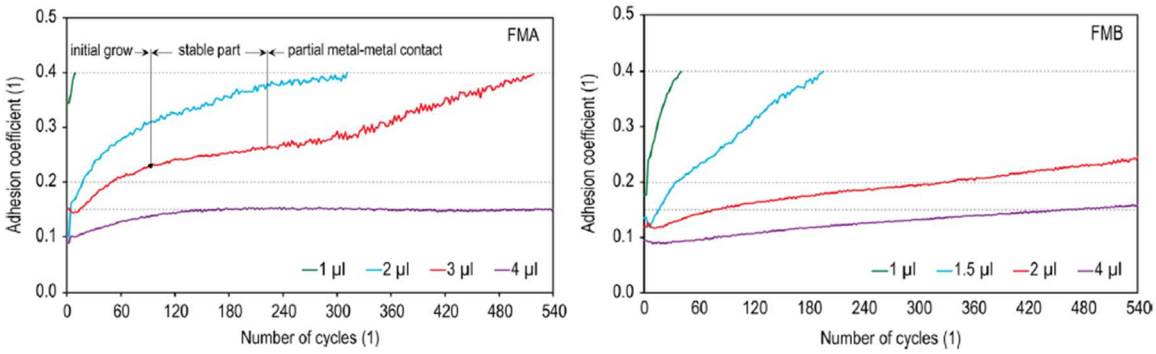

Fig. 15 Effect of applied amount on CoT for FMA and FMB [39]

Recently published standard no. CEN/TS 15427–2–2:2021 [63] defines two types of tests for twin-disc machines whose result is product retentivity, CoT, and the creep curve. It utilises specimens made of actual rail and wheel steel and allows a range of contact

conditions (contact pressure 0.5 – 1.5 GPa, creep up to 3%, speed 0.8 – 1.6 m/s). Each test should be carried out several times and the values should be averaged. In addition, the test for creep curve investigation is described for MTM. It also determines a range of contact conditions which are similar to tests on a twin-disc machine. The experiment starts with an application of TORP followed by a run-in and four tests with increasing creep from 0.25% to 10%. These tests are separated by a "pause" to cool down the samples. It is performed under low speed and pure rolling conditions. This approach to determining product suitability relies on a single, basic criterion that provides limited insight into the product's behaviour.

2.3.2 Carry Distance of TORPs and Transfer Mechanism

Chen et al. [45] investigated the effects of FMs and lubricants on the CoT and assessed their carry distance in the laboratory, which was further compared with field measurements. Frictional behaviour was studied on a twin-disc machine with a wheel disc made of actual wheel steel and a rail disc cut from an actual rail. The speed was 40 km/h and the contact pressure was 751 MPa. The products were uniformly applied by hand followed by rotation of the loaded discs for 60 s. The other approach was to use a nozzle for the injection of substances into the running contact. Solid lubricants (referred to as SL and RTRI-SL) had a positive trend with increasing creep, which is a desirable behaviour and can be applied to the top of the rail. On the other hand, they achieved a CoT value slightly higher than half of that for water. A disc-cylinder device was employed to assess the relative carry distance, which was normalised to the length of the cylinder. The creep value was set around 6 % and

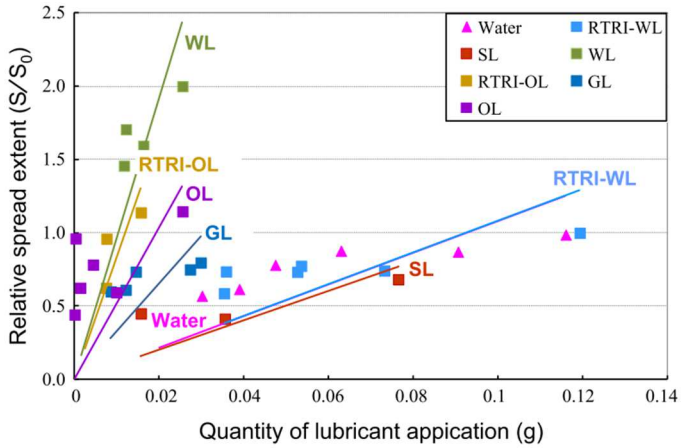

Fig. 16 Effect of amount on relative carry distance (labelled spread extent) [45]

the contact pressure was set to 650 MPa. The authors observed that each substance affects relative carry distance differently whereas FM (labelled WL) had the strongest dependency on amount. see Fig. 16. On the other hand, FM developed by RTRI had the weakest dependency similar to the SL. The examination on the actual rail track did not approve the effect of the amount observed in the laboratory but showed that WL had a significantly longer carry distance than SL and RTRI-WL because the same amount was applied (2 ml

over 2.7 m). Despite its relatively limited carry distance compared to other lubricants, RTRI-WL has shown good performance similar to solid lubricants in reducing lateral force and maintaining brake effectiveness.

Another approach to investigating carry distance is to measure the presence of TORP on the wheel or the rail, in addition to measuring CoT. For this purpose, the band saw was highly modified [64]. The rail was represented by the belt, on which water-based FM was applied in a puddle measuring 4 cm in length and 0.5 mm in thickness. The FM was dyed with a fluorescent dye to allow its detection using laser-induced fluorescence. Three types of wheels were used, one cylindrical and two with transverse radii of 200 and 400 mm. The speed ranged around 30 km/h and the contact pressure was set to 46 and 420 MPa. The authors observed that the cylindrical wheel was separated from the belt by an FM film under unrealistically low contact pressure and they detected FM in the contact band in the fifth imprint. In contrast, the higher contact pressure squeezed the FM out of the contact band, and it was transferred only on the edges of the wheel. In addition, the thickness of FM film in the contact band was under the detection limit (3.4 µm) even at the application place, see Fig. 17. For the crowned wheels, the FM was unable to spread into subsequent imprints because it split evenly (50:50) between the wheel and the rail. The resulting thickness of FM on the wheel was insufficient to reach the counter body and transfer the FM. Aluminium strips were attached to the wheel and the belt to assess the amount of FM in the central part of the contact band. The strips were weighed before and after the pass, which showed that the FM is presented in thickness around 800 nm, comparable to roughness.

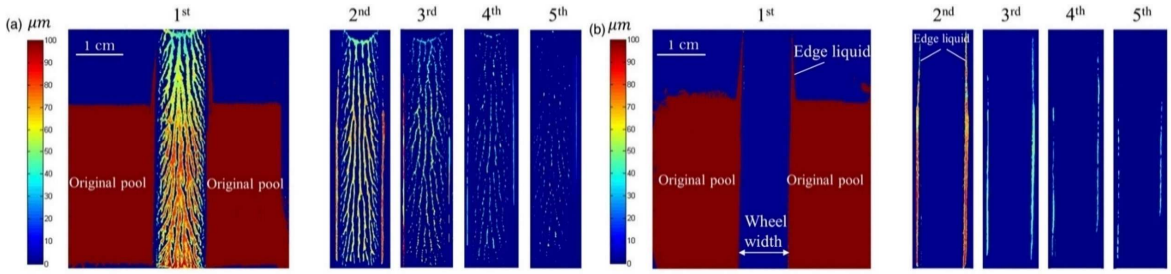

Fig. 17 The film thickness of imprints created by cylindrical wheel: a) low contact pressure, b) high contact pressure [64]

Studies [65,66] employed the full-scale rig to study the pick-up mechanism and carry distance, while the consumption mechanism was also studied on the twin-disc rig. Two water-based FM were examined whereas FM-B was more watery. The micropipette was used to apply FM on the rail in amounts ranging from 130 mg to 780 mg. The abovementioned parameters were assessed based on the CoT and the relative amount that remained on the rail (pick-up mechanism) or wheel (carry distance) after the wheel-rail interaction. In the first interaction, approximately 50% of FM remained on the rail and the ratio increased with further interaction, see Fig. 18a. In the case of FM-B, almost 100% remained on the rail after the third interaction. Carry distance showed a similar pattern, indicating that the transfer of an FM from the wheel was more restricted in later interactions. FM-B reported higher CoT for all tests, consistent with the previous finding. Moreover, FM-

A tended to create strings between the wheel and rail that could lay on the contact band and maintain lower CoT.

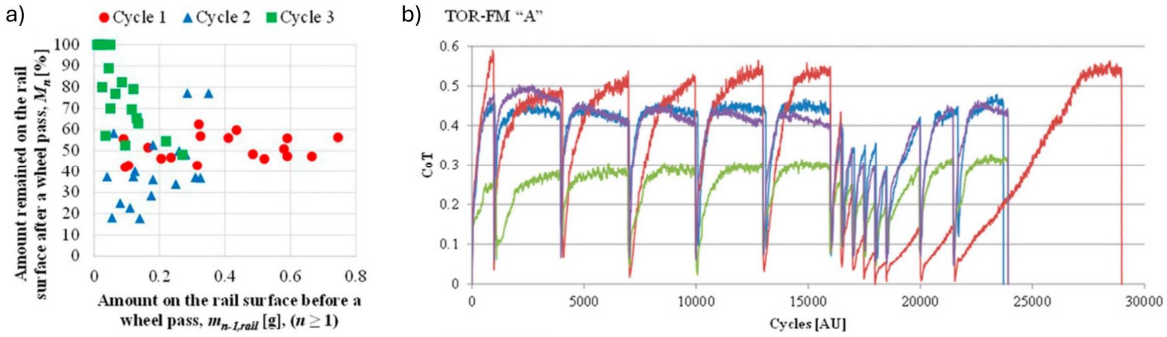

Fig. 18 a) Pick-up ability, b) Consumption of FM [66]

As mentioned, the consumption was tested on the full-scale and twin-disc rigs. The discs were made of wheel and rail steel and the conditions were as follows: contact pressure of 1500 and 900 MPa, speed of 400 rev/min and slip of 1% and 0.5%. The tests began with a run-in phase under dry conditions, lasting 1000 cycles. After that, the 50 mg of FM was applied five times every 3000 cycles, five times every 500 cycles and three times every 1500 cycles. The results from the full-scale rig showed that a higher amount of FM prolonged the restoration time and FM-B reported higher CoT. In contrast, the twin-disc results showed a negligible effect of an amount when the other conditions were the same, see Fig. 18b. However, the higher application rate decreased CoT because it was not fully consumed therefore it was accumulated. The reduction of contact pressure and slip decreased the consumption rate.

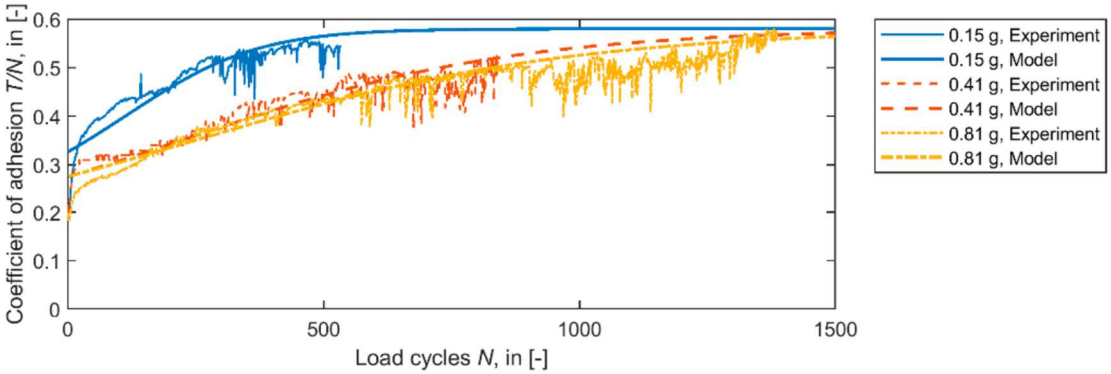

Fig. 19 The effect of FM amount tested on the full-scale facility [67]

Trummer et al. [67] created a model for predicting the evolution of the coefficient of friction in railway operations. It considers three mechanisms – the pick-up mechanism, transfer of TORP and product consumption. The model was parametrized on the experiments conducted on a twin-disc machine and a full-scale facility. The tests on the twin-disc machine were performed under the same conditions as in the previous study [66]. In the case of the full-scale facility, the normal force of 80 kN and slip of 5% were used. Three amounts of FM were applied on the rail at the test beginning. The increasing amount of FM decreased the CoT and it took more cycles to reach the dry level of CoT, see Fig. 19. However, a threshold

amount exists, when it is exceeded, the CoT is not further reduced. It may indicate that the redundant amount is squeezed out from the contact and does not affect the CoT further. The results showed that all three mechanisms may limit the carry distance.

2.3.3 Effect of TORP Compositions on CoT

Several commercial TORPs exist, but manufacturers provide only limited information about their composition. Different components affect performance in various ways depending on their amounts. Galas et al. [40] studied the effect of constituents of water-based FM utilizing a ball-on-disc tribometer MTM. The steel of AISI 52 100 was used to produce the ball and the disc while the disc used for the wear test was made of C45. The tests were carried out under the following conditions: contact pressure 750 MPa, speed 300 mm/s and SRR 5%. The specimens were ultrasonically cleaned in acetone and further run-in until the CoT corresponding to dry conditions was not reached. Various amounts of FM were applied to the disc and were tested under wet and dry conditions. The authors showed bentonite with water maintains intermediate CoT, which is controlled by the percentage amount of bentonite, while the lasting effect (until CoT of 0.5 is reached) is affected by the applied amount. The composition of water and talc reduces the CoT, with the reduction depending on the amount of talc whereas the higher amount may cause critically low CoT. In the case of complex substances, the CoT is mainly affected by water and bentonite while the effect of mineral particles was rather negligible. The authors observed that the presence of water has a significant impact on the behaviour of the substances, see Fig. 20. The substances provide higher and more stable CoT after drying than with the presence of water. In contrast, a study [68] carried out on the high-pressure torsion rheometer showed that FM in wet conditions resulted in a higher CoT than after drying. Moreover, the CoT slightly decreased with increasing amounts of wet FM but when the FM dried out the effect on the amount was significant. The CoT dropped to a level which is insufficient for traction and braking.

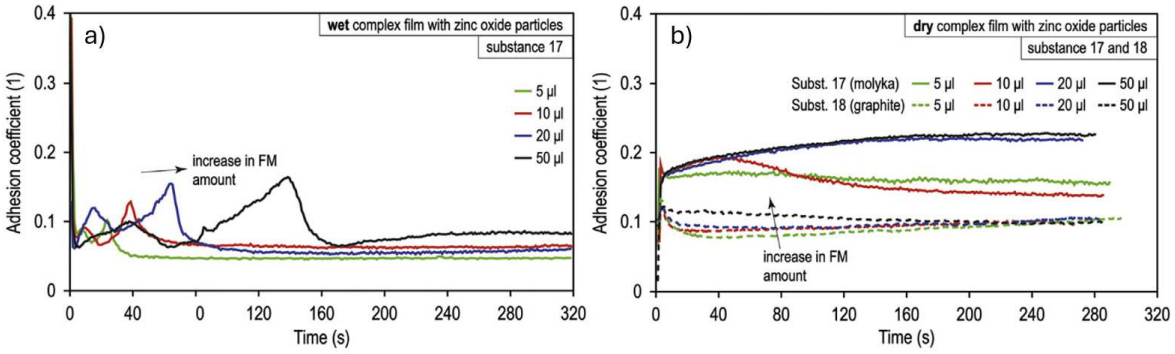

Fig. 20 Different behaviours of the complex substances under a) wet and b) dry conditions [40]

Besides the composition of FM, its viscosity also plays a role, which was studied by Wu et al. [69] employing the twin-disc machine. The specimens were manufactured from the actual wheel and the rail. The contact pressure was 1100 MPa, with a speed of 1.44 m/s and a creep

of 1%. The discs were ultrasonically clean followed by run-in which lasted for 5000 cycles under the same conditions as the following experiment. The FM consisted of water, graphite, kaolin, acrylic-resin emulsion, and sodium carboxymethyl cellulose. The viscosity was altered by changing only the amount of cellulose. Several amounts applied via manual dispenser were examined. The authors found out that the effect of viscosity on CoT depends on the applied amount. Under a low applying amount, FM with high viscosity could produce a lower COA level and a longer retention time, see Fig. 21. Higher amounts of FM led to a lower CoT and repeating application caused over-lubrication of the contact resulting in poor CoT recovery during two minutes. In some cases when FM with lower viscosity was applied, the secondary descent and backflow were observed, which affected the performance of FM.

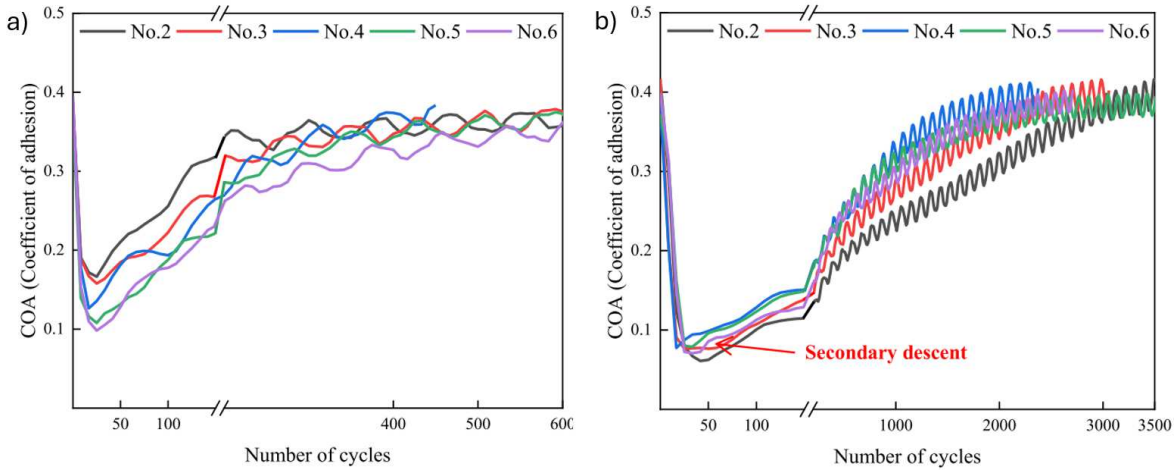

Fig. 21 The evolution of CoT for compositions with different viscosity: a) amount of 5 µl, b) amount of 70 µl [69]

In comparison to the abovementioned study [40], Kvarda et al. [70] used slightly different conditions to investigate the role of different components in TOR lubricant on adhesion behaviour. The main differences are speed 1000 mm/s, contact pressure 800 MPa, SRR 2% and ball and disk made of AISI 52100. The specimens were cleaned with acetone before each experiment and followed by 10 10-minute run-in phase to stabilise the roughness of the surface in 0.1-0.3 µm. The amount of 4 µl was applied in the case of lubricant and 0.5 ml of solution of solid particles to be tested dry.

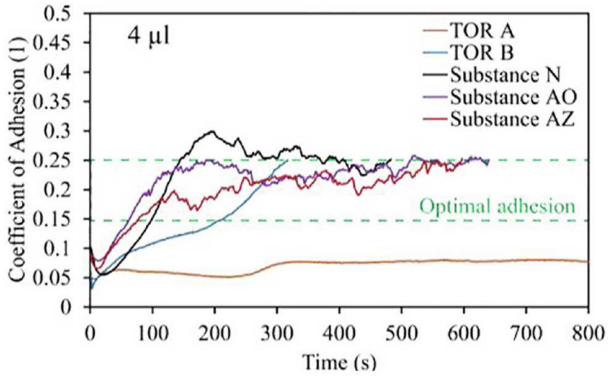

Fig. 22 Comparison of custom-made and commercial TORLs [70]

The results showed that resulting CoT depends on the particle size of alumina and its amount in compositions. When adding solid lubricants, it was found that the alumina content was important to achieve an intermediate CoT rather than increasing the solid lubricant content. Three compositions were prepared and compared with commercial TORLs (TOR A and TOR B), while two parameters were evaluated, the period of intermediate CoT and time to reach CoT of 0.15. The two custom-made substances with a higher content of alumina were best performing when 4 µl was applied as they maintained the intermediate CoT longer, see Fig. 22. The behaviour of commercial TORLs were strongly dependent on the amount while custom-made compositions maintained optimal CoT longer when larger amount is applied.

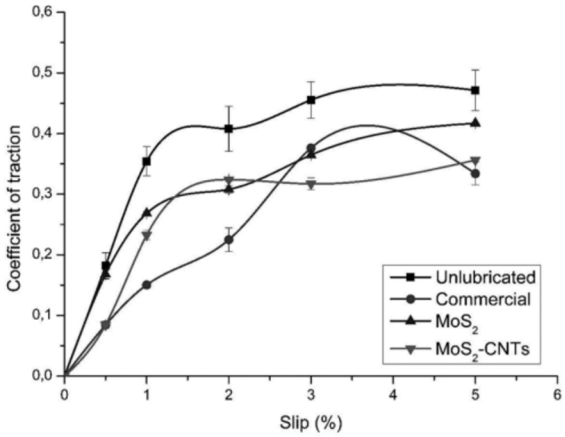

Fig. 23 The creep curves of commercial and developed bars [71]

The study [71] investigated the composition of solid sticks and utilized a twin-disc machine with discs extracted from the actual wheel and the rail. The contact pressure was 1.1 GPa and slip varied from 0 to 5%, while wear tests were carried out for 1 and 5% of slip. The three types of solid sticks were studied – one commercial, one with MoS_2 and one with MoS_2 and carbon nanotubes (MoS_2-CNT) and were applied continuously. The results showed that MoS_2-CNT is the best performing as it maintained the intermediate CoT similarly to the composition only with MoS_2. The commercial solid stick reported a slower rising CoT until a slip of 3% was reached and a downward trend was observed thereafter, see Fig. 23. The CoT was reduced by more than 10% compared to unlubricated tests using a solid stick with nanotubes and these results were achieved with less than half of MoS_2 in the matrix compared to commercial solid stick. However, the resin composition and particle size distribution of MoS_2 would play a role.

2.3.4 Curve Squeal Noise

Liu et al. [15] investigated the effect of TORPs on the squealing noise under several rolling speeds (100 – 800 rpm) and angles of attack (0 – 25 mrad). TORPs were applied by a brush evenly on the wheel disc. For FM, approximately one hour of drying time was allowed to form a film. In contrast, for TORL, the test rig was operated for about 30 seconds to remove

any excess TORL. The authors observed that the lateral force decreased more for TORL and TORP tended to eliminate or significantly reduce the negative slope of the creep curve. However, the squealing noise was still present in some cases. The sound pressure level (SPL) rose with angle of attack (AoA) and rolling speed under lubricated conditions, see Fig. 24. In some cases when the TORL was applied, the squealing noise became more tonal.

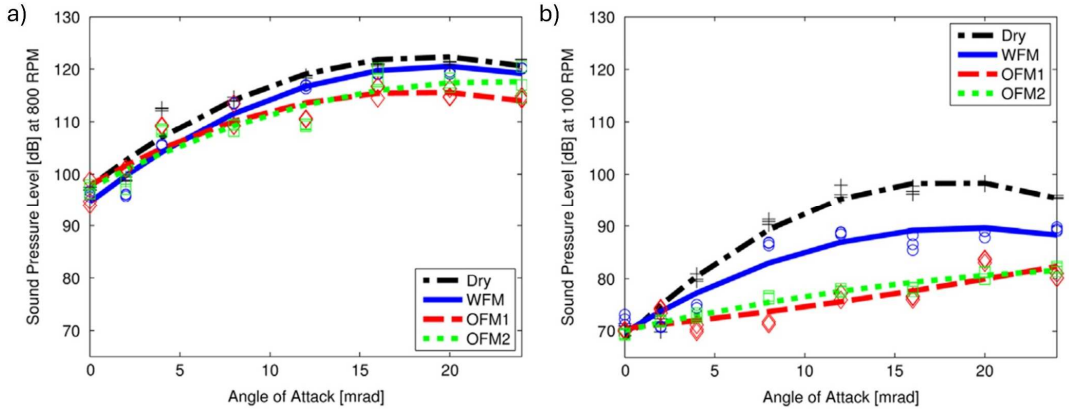

Fig. 24 SPL of various conditions for speeds: a) 800 rpm and b) 100 rpm [15]

Galas et al. [32] studied the effect of TORLs amount on the SPL and its connection with CoT. The twin-disc machine was used and experiments were performed under the following conditions: contact pressure of 0.8 GPa, speed of 1 m/s, SRR of 8% and AoA of 4°. The TORL was applied to the contact path via micropipette. The results showed that TORLs significantly reduce SPL and CoT, with larger amounts providing a longer duration of reduction (Fig. 25). However, larger amounts led to critically low CoT immediately after application, potentially causing braking issues. In contrast, smaller quantities can decrease both SPL and CoT without the risk of braking problems. When the TORL became ineffective, the SPL began to increase rapidly.

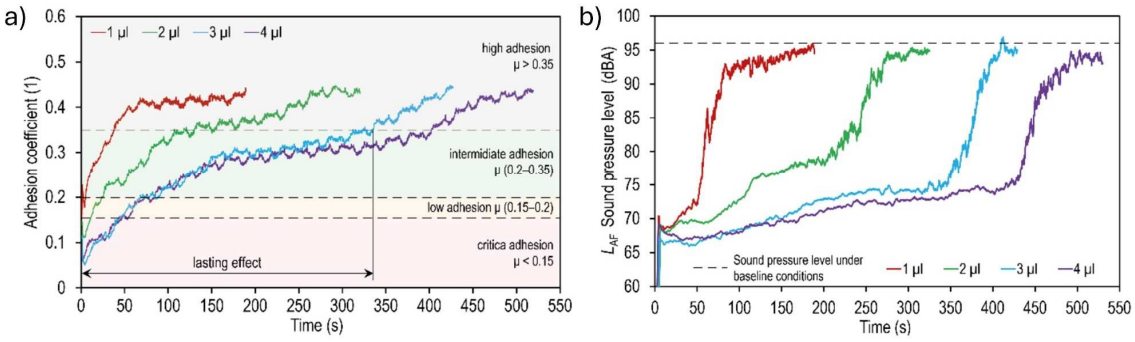

Fig. 25 Effect of TORL amounts on a) CoT and b) SPL [32]

The study [12] aimed at RH's effect on the CoT and squeal noise utilising a twin-disc machine as in [15]. The authors observed that higher RH reduces the CoT and decreases the critical creep, indicating a shift in the saturation point. Additionally, higher RH increases the probability of squeal noise occurrences, see Fig. 26. The study further found that squeal events are triggered when the negative lateral rolling contact damping exceeds the structural damping.

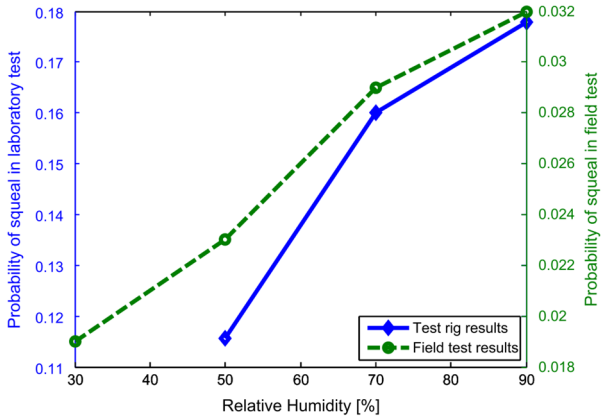

Fig. 26 Probability of squeal in different RH [12]

2.3.5 Similarity of Experimental Approaches

Conditions in laboratory devices are significantly different to those in the wheel-rail contact, therefore study [72] performed a comparison of lubrication parameter (lambda) for smooth and rough surfaces lubricated by water and oil used as a rail gauge corner lubricant. The tests were performed under the following conditions: speed 1500 mm/s, contact pressure 700 MPa and SRR 0-100%. Ball roughness was Ra=0.02 µm and disc roughness was Ra=0.01 µm (smooth) and Ra=0.15 µm (rough). Each test was performed on a new pair, which was ultrasonically cleaned in toluene and dried. Before the test, the 3-minute run-in with the intended lubricant (fully flooded conditions) was carried out to minimize any running-in effects. It was shown that higher roughness significantly decreased the lambda parameter for both cases (MTM and wheel-rail contact), while similar values were obtained for almost ten times lower rolling speed of MTM than wheel-rail rolling speed, see Fig. 27a. The higher roughness results in higher CoT when the contact was lubricated by water whereas remained almost the same for the oil, see Fig. 27b. In the case of dry conditions, the CoT varied between 0.7 and 0.8. When the SRR was between 0 and 35%, the smooth disc resulted in a higher CoT, while the rough disc had a higher value above 35%.

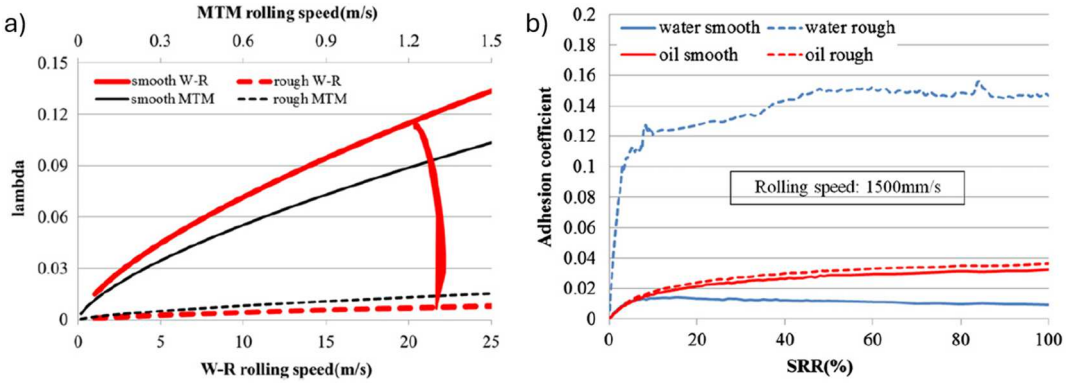

Fig. 27 a) Lambda value for MTM and wheel-rail and b) creep curve [72]

Buckley-Johnstone [47] investigated the similarities between a twin-disc machine and a full-scale facility in terms of wear rate and evolution of CoT (retention). The full-scale facility

was operated under 1500 MPa of contact pressure, creep of 2 % and a speed of 40 mm/s. Tests on the twin-disc machine were carried out under similar conditions, only the speed was set to 1 m/s. The wear tests were conducted under dry conditions and with FM applied every 250 cycles. In the case of retention, the FM was evenly applied on the rail of the full-scale facility by a brush and 0.1 g of FM was applied on the rail disc before the test. The results showed that a correlation between the wear rate from the full-scale facility and the twin-disc machine exists, but some assumptions were made, see Fig. 28. The higher wear rate with an FM was observed for the full-scale facility, which may be caused by a proportionally smaller amount ending in the contact. The twin-disc machine reported lower CoT with FM compared to the full-scale but the evolution is similar.

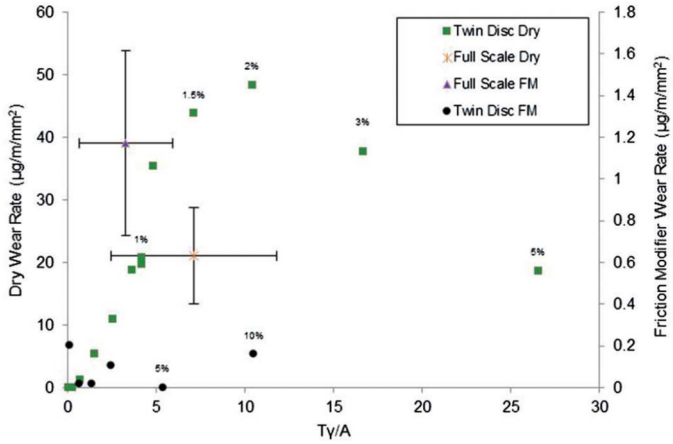

Fig. 28 Wear rate comparison between full-scale facility and twin-disc machine [47]

2.4 Field Measurements

2.4.1 Effect of TORP on frictional properties

Experiments with trains or under operation are expensive and time-demanding, therefore they are not as common as laboratory tests. Oldknow [73] investigated the effect of water-based FM on lateral/vertical (L/V) ratio characterising frictional properties in wheel-rail contact. The study was performed at a track with a radius of 300m while the FM was applied on the top of the rail using a wayside application unit. It should be noted that the gauge face was lubricated during the trial. The L/V ratio reported a significant scatter ranging from 0.1 to 0.8, with a typical value around 0.4. The trailing axles reported a lower L/V ratio than the leading and the difference was larger and clearer when the rain was presented. The typical value also increased especially for the leading axle. The FM reduced the L/V ratio and decreased its variability, resulting in a typical value of around 0.2. The distribution of L/V for the first 50 leading axles can be seen in Fig. 29. Slightly lower values were observed on the iron ore line where the fully loaded train was utilized to assess the CoT [33]. In the first

run, the CoT was too low causing the train to be unable to continue running, which was due to an excessive amount of FM on the rail. The combination of rain and a FM reduced the L/V ratio to a range of 0.1 to 0.4, which is lower than that observed without the FM [73]. On the other hand, the most frequent L/V ratio was shifted to a lower value compared to the dry FM condition.

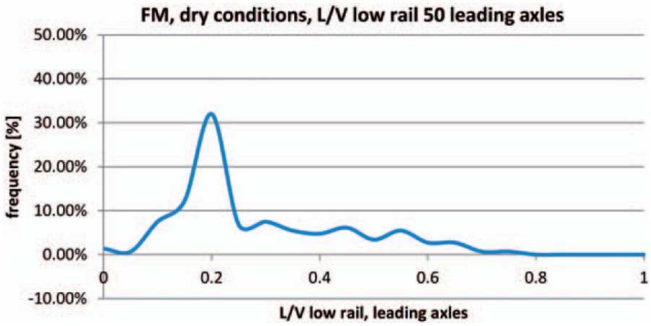

Fig. 29 L/V values distribution corresponding to the first 50 leading axles [73]

Matsumoto [74] studied the optimal application interval of an FM. An onboard spraying unit was mounted behind the last axle of a train, and the applied amount was varied by changing the number of trains spraying FM on the low rail. The L/V ratio was recorded on the low rail of a curve with a radius of 130 m. Fig. 30a shows that one spraying train was insufficient, as the L/V ratio varied from 0.2 to 0.8. Additionally, at the beginning of the trial, the effect of the FM was negligible. Although the L/V ratio decreased after application, the lowest values were recorded only for the second train pass, after which the ratio increased again (see Fig. 30b. When the amount of FM was doubled, the L/V ratio stabilized between 0.2 and 0.4, indicating a substantial improvement. Similar results were obtained in the study [58], where the CoT decreased immediately after an application and gradually increased with train passes.

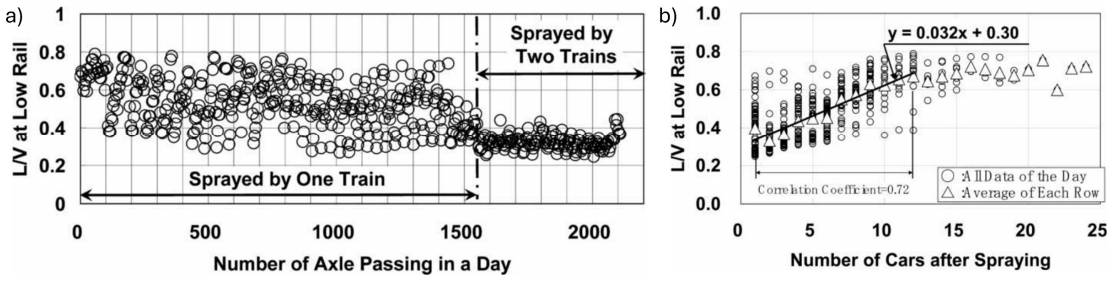

Fig. 30 a) Effect of applied amount on the L/V ratio, b) Correlation between L/V and number of cars after spraying [74]

Galas et al. [32] conducted braking tests with a tram to assess the effect of varying TORL (top-of-rail lubricant) amounts on braking distance. Three different amounts (4, 2, and 1 gram per single rail) were tested, with each test conducted a week apart to ensure dry conditions as a reference. Higher amounts of TORL significantly prolonged the braking distance, see Fig. 31. Notably, the run immediately after application did not result in the worst braking performance; the prolongation was slight or almost negligible. Subsequent runs showed worse performance as the TORL spread along the rail and onto the wheels.

After three runs, the TORL began to be consumed, resulting in a reduction in braking distance with subsequent runs. Only the application of 1 gram of TORL did not affect the braking distance.

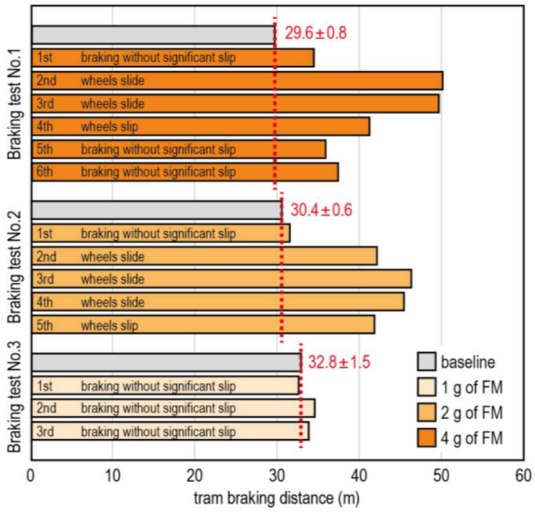

Fig. 31 The braking distance for three applied amounts of TORL [32]

2.4.2 Carry distance of TORPs

Carry distance indicates how far a TORP spreads from the application site, which is important for the distribution of the wayside application unit along a track. Each TORP reaches a different value. A study [75] compared two TORPs, both were classified as FM, but FM-B dried slowly and might be a hybrid TORL. At first, the wayside unit was installed on the low and the high rails before the sharp curve with a radius of 400 m and a four times higher amount (1 litre per 1000 axles) than recommended by a supplied was applied. Samples were collected via cotton swabs dipped in solvent and further analysed by energy dispersive X-ray. The authors found that FM-A had a poor carry distance (70 m) compared to FM-B (450 m) when the samples were taken from the rail, which was significantly lower than the manufacturer claimed. Similar results were obtained on the tangent track, where 15 ml of FM was manually applied with a brush over a distance of 7.4 meters. Different situations occurred when the samples were collected from the wheel. The FMs were detected on the running surface of the wheel even after three kilometres, but FMs were mainly located on the edges of the contact band, preventing it from coming into contact until the contact band changed. Therefore, the samples were collected only from the contact band, the difference can be seen in Fig. 32. It showed a significant reduction in carry distance, which was comparable to that recorded from the rails.

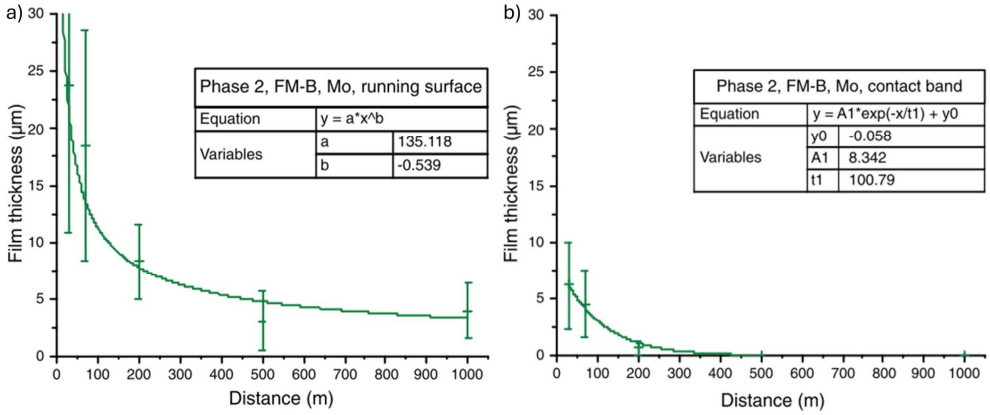

Fig. 32 Film thickness vs distance: a) evaluated from whole wheel cross-section, b) evaluated from contact band [75]

The fluorescently dyed FM was used to investigate the carry distance in the field [64]. A wayside top-of-rail application unit supplied an FM at the rate of 2.8 ml per 7 axles on the railhead. The axles picked it up and further transferred it. The authors observed that film thickness was larger when the rail was pre-conditioned by 33000 axles, but the carry distance assessed based on film thickness was the same compared to the first train pass. The FM was detected on the railhead over the length of 150 m, while on the contact band, it was only found over 100 m. In contrast, the FM appeared again at the curve, which was located about 500 m downstream from the application unit, see Fig. 33. Moreover, it was observed on the railhead more than one kilometre downstream from the last point of observation. The authors explained that the FM near the contact band on the wheel is transferred or consumed over a few hundred meters of the tangent track due to bogie hunting. When the bogie reaches a curve, the location of the contact band changes, causing the FM to come into contact with the track and be deposited.

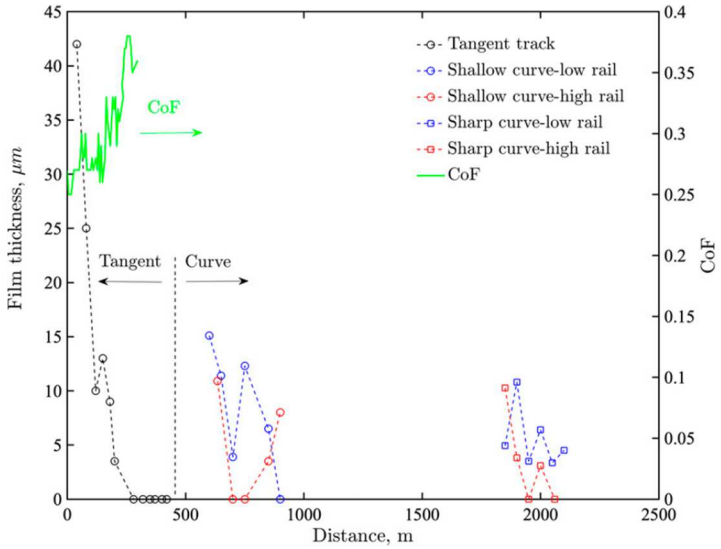

Fig. 33 FM film thickness and CoT measured at several distances from the application site [64]

2.4.3 Curve Squeal Noise

Eadie et al. [8,29] investigated the curve squeal in the field as it is a loud and annoying noise. Several rail systems (tram, metro and freight) were accomplished in the studies, where each had a specific noise manifestation varying in the specific frequencies and the absolute SPLs differed by about 20 dBA. The application of FM reduced the average SPL by about 10 dBA across all systems, see Fig. 34a, but only for systems with the highest overall noise levels, the noise tends to be reduced across a broader part of the spectrum. The main reduction was in a range from 500 Hz to 2000 Hz but it may differ from case to case. In some cases, the reduction of flange noise was observed although the top of the rail was coated, see Fig. 34b. The heavy haul freight lines require gauge face lubrication in addition to a TOR unit to fully control noise because the higher lateral and flanging forces are presented in sharp curves.

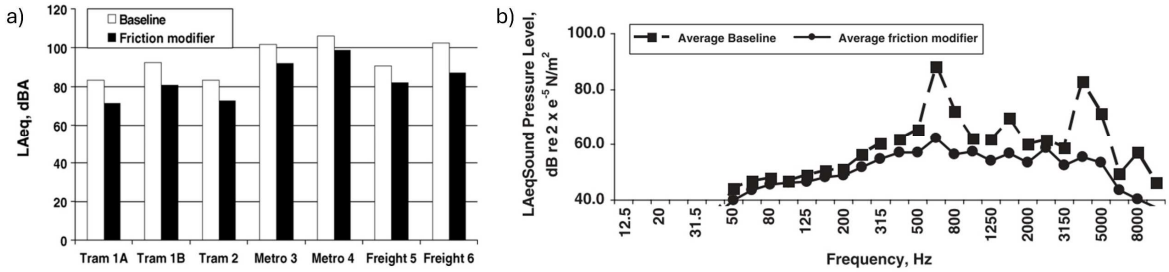

Fig. 34 a) Average sound pressure level reduction [8], b) Spectral change after an application of FM [29]

In contrast to above mentioned, Curley et al. [76] studied a heavy haul curve with a radius of 290 m and observed that TOR friction modification on the low rail was not an effective method for reducing noise. The authors tested various scenarios using gauge face lubricant and TORP in different dosages, either individually or in combination, with different treated rails. The application units were initially located in the middle of the curve, and in the second phase, the gauge face lubrication unit was placed at the start of the curve. The best results were achieved when the gauge face of the high rail was lubricated while simultaneously treating the top of the rail with TORP. Vibration data indicated that most noise events originated from the high rail, explaining why friction modification on the low rail was ineffective. This indicates the need for initial measurements to determine the noise source and select an appropriate friction adjustment method.

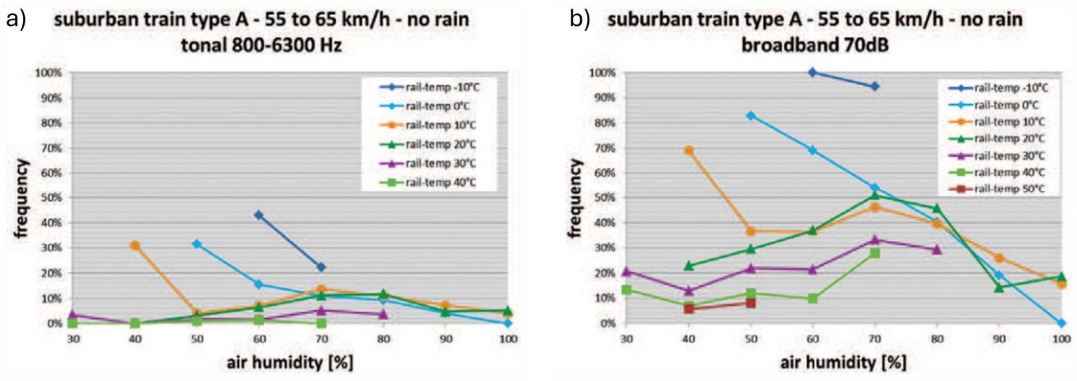

Fig. 35 Frequency of occurrence of a) squeal noise and b) broadband noise [14]

The effect of weather conditions on the curve squeal was studied by Maly et al. [14] on the suburban railway curve with a radius of 230 m for 11 months. The authors observed that tonal and broadband noise occurrences are significantly reduced during rainy conditions and when rail temperatures are below the dew point. The highest values were recorded for RH in the 60% to 80% range, see Fig. 35. As rail temperatures increase, the occurrence of both noise types decreases, with almost no occurrences at rail temperatures above 30 °C. The sound power level is slightly lower at higher rail temperatures but tends to increase with higher humidity. At temperatures below 10 °C, the sound power level is notably higher when air humidity is low.

2.5 Portable Tribometers

Portable tribometers are devices that are utilized to assess CoT on the actual tracks whereas some of them can be used also in the laboratory on the actual rail. These devices were developed as an alternative approach to instrumented trains or bogies, which are expensive and time-consuming to use. The main division may be made according to the condition of the contact with the rail to fully sliding and rolling-sliding. Other criteria include the level of simplification, the method of inducing creep, and whether the tribometer is moved or fixed to the rail.

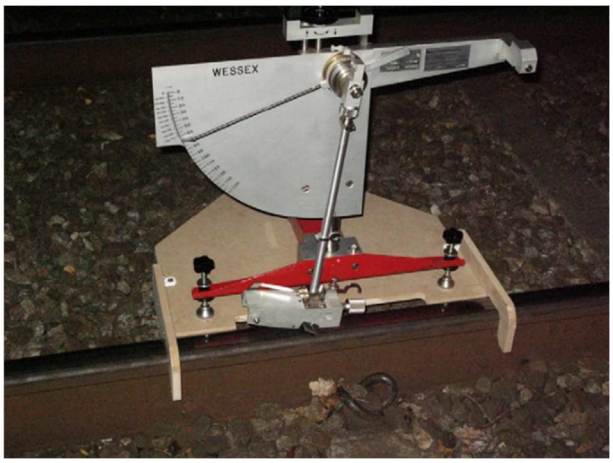

Fig. 36 The pendulum tribometer [77]

One of the simplest devices is the Pendulum (Fig. 36), which works on the same principle as the Charpy impact test [77]. A certain amount of kinetic energy is lost as the slider pad comes into contact with the rail surface and slides over it. The energy lost is measured and further converted into a coefficient of friction. The main advantage of this approach is a fast assessment of CoF, but the sliding pad is made of rubber, which is not highly representative. The formula used to convert the energy lost has developed over time because it was found that it is not accurate enough for all conditions. At first, it was calibrated to the results from

the twin-disc machine [78] and further to the tribometer train [79]. Moreover, the obtained value depends on the state of the rubber and its type.

The other device is the FricWear tribometer (Fig. 37), which was designed to measure the CoF and wear constant in both field and laboratory conditions but it is adapted to the rail [80]. The tribometer operates under fully sliding conditions as the wear probe loaded with dead weights is pulled by a motor while the force is simultaneously measured via a force sensor. The wear probe is made of rail steel, while for friction tests, bearing steel may be used. The maximum contact pressure is 2.1 GPa and the sliding speed is 30 mm/s. The authors claimed that the limited measuring distance (approximately 15 cm) is a disadvantage but on the other hand, it allows them to measure the local CoF.

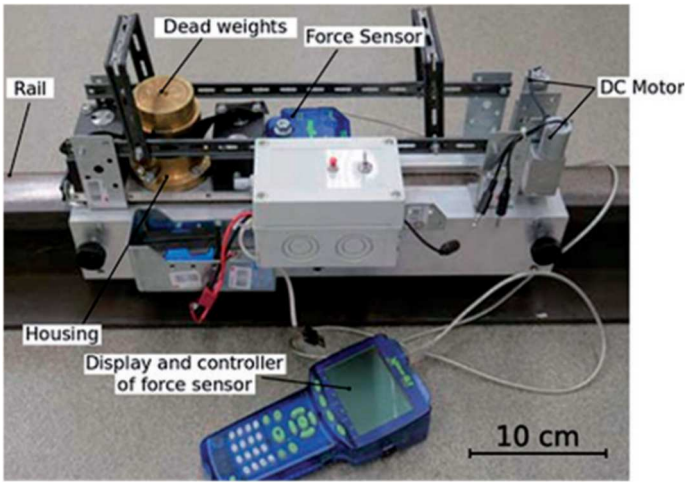

Fig. 37 FricWear tribometer [80]

TriboRailer [81] is a car-pushed tribometer (Fig. 38), which acquires CoT from the TOR and gauge side simultaneously for a large distance. Both normal and friction forces are measured by a specially developed biaxially-sensitive load cell. It consists of a twin-hulled chassis, and each contains four wheels – the outermost ones are guiding and the middle ones measuring. The device can induce only 2.5% creep by yawing the measuring wheel. TriboRailer can determine an adhesion curve for a low slip regime.

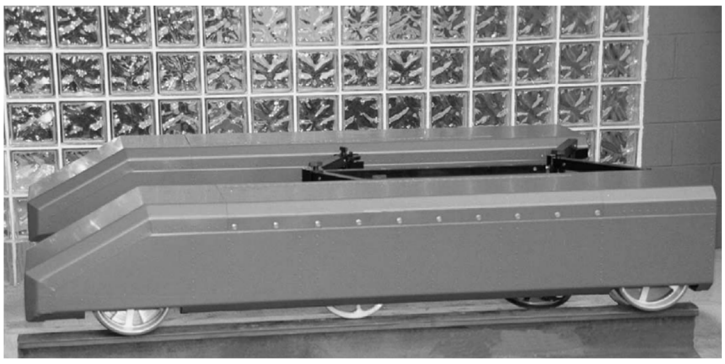

Fig. 38 The TriboRailer [81]

Another type of tribometer is a Hand-pushed tribometer, see Fig. 39. The device uses the brake to develop slip in the contact. The commercial tribometer measures top-of-rail and

gauge-face friction [33,81]. The contact pressure is induced by a spring, which a screw can adjust. Three seconds measuring sequence starts, while a steady speed is reached. The braking torque is increasing. When the measuring wheel starts sliding, the braking torque is reduced, and longitudinal force is acquired. At the end of each sequence, the CoT is displayed. The device does not record slip and CoT during the whole measurement. The custom-made hand-pushed tribometer (TriboMetro FR 101) [82] uses the same principle of inducing creep into contact as the previous one. The spring-loaded wheel creates 1 or 1.2 GPa contact pressure and is braked. The device has a personal computer storing data and controlling the measurement via an acquisition card. Once the measurement is finished, the CoT is reported together with the adhesion curve.

Fig. 39 The Hand-pushed tribometer [33]

The latest generation of field tribometers includes the Hand-operated (HO) tribometer [83–85], also known as OnTrak [86], see Fig. 40. In this device, creep is induced laterally by rotating the measuring wheel at a specific AoA, similar to the TriboRailer. Measurements can be performed with either a constant or changing AoA, which can be set to achieve approximately 16% creep, according to [85,86]. Thus, the HO tribometer operates in a low-creep regime. While changing the AoA allows for evaluating the creep curve in a single pass, this mode is not reliable. Additionally, using controlled slip in the lateral direction to build a creep curve may be considered less representative.

Fig. 40 Hand-Operated Tribometer [85]

2.5.1 Tribometer Comparison and Influencing Factors

The results from above mentioned tribometer were compared to some of the other tribometers. Lundberg et al. [33] employed fully loaded IORE to assess the CoT before and after the application of FM that was applied manually using a brush. The measurement with the tribometer was conducted before the train passed. The tribometer significantly overestimates the CoT, as shown in Fig. 41. Under unlubricated conditions, the CoT was overestimated by a factor of 2.2, while under lubricated conditions, it was overestimated by a factor of 1.4. The authors attributed the discrepancy to the scale factor, which causes border effects that increase the frictional force on the small wheel, and to the different contact pressures (1 GPa for the tribometer and 1.5–2.7 GPa for a train).

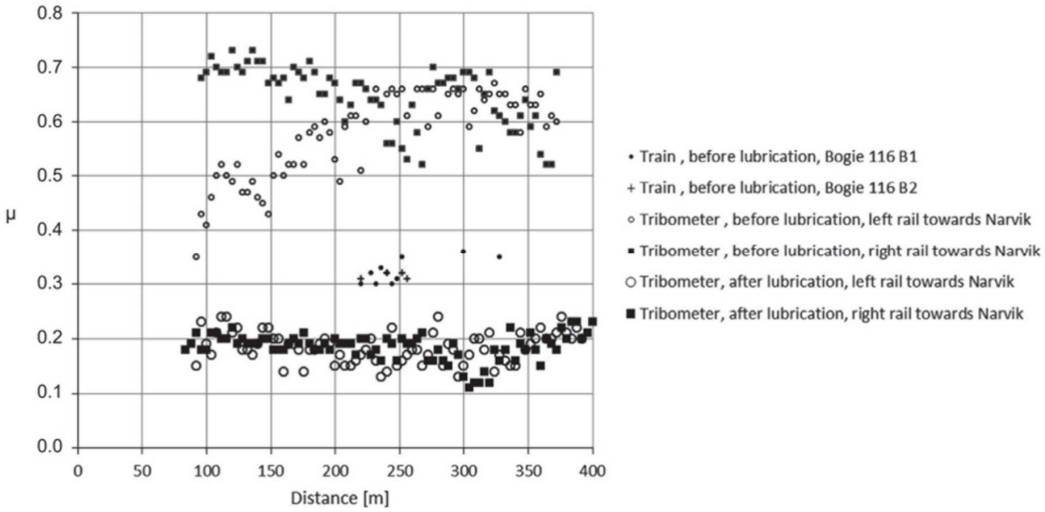

Fig. 41 The comparison of the Hand-pushed tribometer and IORE locomotive [33]

The pendulum was compared to other testing methods, like hand-push tribometer, full-scale facility and twin-disc machine [78]. The authors observed that the pendulum and hand-push tribometer show the same relationships for different interfacial conditions, while the pendulum is more sensitive to different contaminant types. The difference in CoF was greater between the various conditions. The pendulum overestimates the CoT compared to the hand-push tribometer and laboratory rigs. In the case of the tribometer, the difference is not large, but for other rigs it is, see Fig. 42. The authors assign the difference to the different contact pressures, full sliding conditions and the material of the sliding pad.

As was mentioned, the contact pressure affects the CoT, which was observed in many studies utilizing portable tribometers [81,82,86,87]. A decreasing trend of CoT with rising contact pressure was observed across many conditions, including dry contact, water FM, TORL, and lubricants. Moreover, the study [87] observed that the rate of decrease varies depending on the geometry of the measuring wheel and the third body layer. It is significant for dry contact and almost negligible for lubricated contact reporting low CoT.

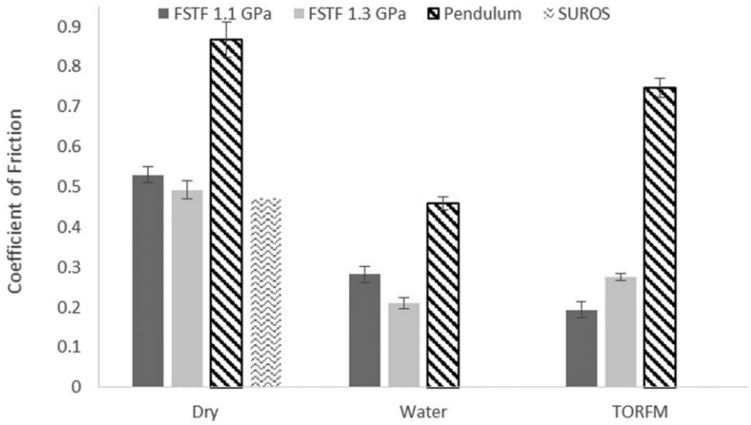

Fig. 42 The comparison of the pendulum to the full-scale facility (FSTF) and twin-disc machine (SUROS) [78]

Harrison [88] investigated how the state of the measuring wheel affects the results. He defined four cases as depicted in Fig. 43a starting from clean states that transfer to the conditioned ones. The results showed that CoT increases during the transition from case 1 to case 4, see Fig. 43b. Once the measuring wheel was cleaned (case 2), the first readings were significantly higher than that in case 1. Moreover, the CoT reached the value of case 4 after several passes. When the wheel remained conditioned and the rail was cleaned (case 3), the first readings were similar to that in case 1 but the gradient was higher. It indicated that a small amount of third-body residue was present on the wheel letting it develop higher readings more quickly while the majority remained on the rail. Therefore, case 2 is a suitable method to assess friction conditions on the rail.

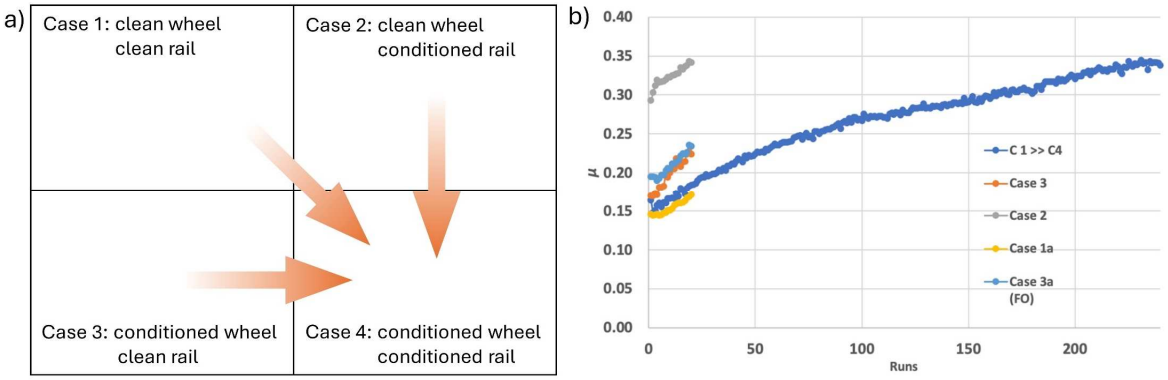

Fig. 43 a) Nominal states of wheel and rail, b) evolution of CoT for different states [88]

3 ANALYSIS AND CONCLUSION OF LITERATURE REVIEW

3.1 Analysis of General Knowledge

Friction management has been investigated for decades and the first study was carried out in Vancouver with a solid stick [20]. Further studies are focused on liquid TORPs, mainly on water-based FM [24,33,34,57,58,65–67,82] and TORLs are rather neglected [32,60,70], similarly as solid sticks [42,59]. The main purposes of the TORPs are to provide a positive creep curve and to maintain the intermediate CoT, which results in a reduction of wear [19,26,27], noise [8,15,31], lateral forces [18,21,22] and so on. They also have downsides like prolonged braking distance [32,33] and a risk of very low CoT due to water contamination [35].

Many studies performed time tests of TORP where a significant drop in CoT was observed immediately after the application followed by a gradual increase. The drop depends on the composition of TORP [62,70], its viscosity [69] and applied amounts [32,39,70]. Moreover, it respects the application history connected to a consumption rate [61,65,66]. When a proper amount is applied, the CoT may reach the value before the application [65,66], otherwise, the CoT gradually decreases while maintaining the same dosage interval [61]. The lower contact pressure and slip report a slower consumption rate [24,65,66]. The study [67] showed that a higher amount prolongs the time of consumption but a curtain limit exists over which no further prolongation is provided. Other studies [39,40,69,70] observed similar dependency but no limit was reached which may be due to significantly lower amounts.

Besides time tests investigating CoT, the other important parameter is carry distance defining the distance where the TORP can be spread. It can be studied in the field [64,75] or the laboratory utilizing a full-scale facility [65,66] or special devices [45,64]. The values significantly vary depending on the detection method and the type of TORP. Water-based FM reports a shorter carry distance than oil-based TORL [75]. Only a small amount of TORP is presented in the contact band and gradually consumed while the majority is located outside of the wheel-rail contact band [64,75]. These reservoirs on the wheel can last for several kilometres [75] and they are consumed in further curves because the contact band is changed [64].

Curve squeal occurring in sharp curves can be categorized into squeal noise and flange noise, with characteristic frequencies ranging from 400 Hz to 5 kHz [9] and from 5 to 10 kHz [8], respectively. Each rail system has slightly different characteristic frequencies and absolute SPL [8,29]. Laboratory measurements reported an SPL reduction of 20 dB [15,32], but in the field, only 10 dB were observed [8,29]. In some cases, TORP application led to a

reduction in flange noise, even though it is generated at the gauge corner. Curve squeal is also influenced by weather conditions, with the dependency of sound power level on relative humidity varying with rail temperature [14]. Higher relative humidity increases the probability of squeal [12].

3.2 Experiment Design in the Laboratory

There are several types of experimental devices which can be used to investigate the wheel-rail contact in terms of wear, RCF and frictional properties. The main difference is the level of simplification. The full-scale facilities with actual wheels or rails are on the one side while pin-on-disc devices with fully sliding contact are on the other side. The full-scale facilities utilizing wheel and rail have a good representation of the actual contact, but the speed is significantly limited (40 mm/s) [47,65,66]. Higher speeds (up to 90 km/h) can be achieved when the rail is replaced by a wheel [48,60].

The twin-discs machines are widely spread and mainly custom-made devices, which differ in geometry of the specimens creating a line [42,59,61] or a point contact [32,62]. The discs are usually cut from the actual wheel and rail [42,59,61], made of similar steel [39,58] or made of bearing steel [62]. These devices have still a good representation of the actual contact, as the specimens are cut from the wheel and the rail, but the contact size is significantly smaller. Moreover, the operation is cheaper, and the specimens can be easily replaced with new ones. The experiments are carried out under various conditions (see Tab. 1) while contact pressure ranges around 1 GPa and the most common speed is 1 m/s, but a significantly higher speed (40 km/h) can be found [45,58]. The creep values depend on the test: the creep curve test utilizes sweep from 0% and the test with constant creep uses creep around 1%, where the saturation point is located, and the wear is smaller.

The ball-on-disc tribometer or MTM is another device with rolling-sliding contact representing the actual wheel-rail contact pretty well. Compared to twin-disc machines, the MTM is a commercial device. The specimens are typically made of bearing steel AISI 52100, but the disc can also be made from steel similar to that used for wheels or rails [40]. The contact pressures do not vary as for twin-disc machines (see Tab. 2), but the speed has a wide range.

The specimens are usually cleaned before experiments with a solvent that may be acetone [40,70] or toluene [72], additionally, some researchers utilised ultrasonic baths [39,40,69,72]. A Run-in process was performed before the main experiment in many studies, see Tab. 1 and Tab. 2. It aims to stabilize CoT [42] or the roughness [40], to reach CoT of dry conditions [39,40] or to minimise any running-in effect [72], like a change of geometry. Most of the run-ins were performed under dry conditions but each researcher defined his

criteria to stop the run-in. It may be the time, the number of cycles, the reached CoT level or the CoT stabilisation.

Tab. 1 Experimental condition used on twin-disc machines

Ref.	Contact pressure (MPa)	Speed (m/s)	Creep (%)	Run-in	Application method	Amount
[32]	800	1	8	until the dry level of CoT was reached	micropipette	1-4 µl
[42]	900	1	–	until CoT stabilisation	–	–
[45]	751	11.1	0 – 25	–	uniformly by a hand	0.2 and 0.7 g
[47]	900, 1500	1	0 – 5	–	brush, spray	0.1 g
[58]	670	11.1	0 – 12	5 minutes, dry conditions	–	–
[59]	470	0.3, 1	0.1 – 0.5	3000 cycles under dry conditions	–	–
[61]	1500	1	1	4000 cycles under dry conditions	brush or cotton swab	0.05 g / 500 cycles
[62]	500	–	0.5, 11	–	–	20 µl when CoT > 0.3
[65–67]	900, 1500	1	0.5, 1	1000 cycles under dry conditions	syringe	0.05 g / 500, 1500, 3000 cycles
[69]	1100	1.44	1	5000 cycles under various conditions	manual dispenser	5 – 10 µl
[71]	1100	–	0 – 5	–	–	–

The methods for applying TORPs differ in both the laboratory and the field. The hand application using brush [82] or rolled [29,33] is used in short-term trials while wayside bars [8,29] or on-board spraying systems [24,74] are utilised during long-term trials. In the laboratory, TORPs can be applied precisely using a micropipette or less precisely using a brush or spray. Most of the studies started the measurement immediately after the application but a redistribution may be employed [39]. The TORPs are applied at once before the experiment or several times during the experiment while the conditions for reapplication used to be a number of cycles, time or level of CoT. It also depends on the type of experiment. The applied amounts range from several µl [32] to tenths of grams [45].

Tab. 2 Experimental condition used on ball-on-disc tribometer

Ref.	Contact pressure (MPa)	Speed (m/s)	Creep (%)	Run-in	Application method	Amount
[39]	750	0.3	1 – 10	until CoT stabilisation on a dry level	micropipette; redistributed over several cycles	1-4 µl
[40]	750	0.3	5	until CoT stabilisation on a dry level	micropipette	5, 10, 20, 50 µl, 1 ml
[70]	800	1	2	10 minutes under dry conditions	micropipette	2, 4, 6 µl
[72]	700	1.5	0 – 100	3 minutes with lubricant	–	fully flooded

3.3 Portable Tribometers

There are several ways to assess the friction properties on the railway. The most repetitive measurement is with an instrumented train [33], which ensures the actual contact conditions but the experiments are expensive and time-consuming. Therefore, portable tribometers are a suitable alternative. Experiments with them are cheaper, faster, and may be performed during operation. Some can be used in the laboratories, although they offer lower contact representativeness.

The simplest device is the Pendulum [77–79], which operates on energy loss principles. It overestimates the CoF [78] compared to twin-disc and full-scale rigs, likely due to the rubber pad sliding over the rail. Another device with fully sliding contact is the FricWear tribometer [80], which can determine both wear and CoF. Its probes are made of rail or bearing steel, and a dead weight induces a maximum contact pressure of 2.1 GPa.

Other tribometers operate under rolling-sliding conditions, which are closer to the actual conditions and thus better options. TriboRailer [81] is a car-pushed tribometer capable of recording CoT on TOR and gauge side over long distances. It induces creep by yawing the measuring wheel while measuring normal and lateral forces, and it can also determine the creep curve. In contrast, the Hand-pushed tribometer [33,81] induces creep by braking the wheel, recording CoT only when creep occurs. It measures normal and longitudinal forces and can assess CoT on TOR or the gauge corner. The custom-made hand-pushed tribometer [82] can provide an entire creep curve. However, hand-pushed tribometers tend to overestimate CoT because measurements are taken under high creep.

The newest device is the HO tribometer [83–85], which attaches to the rail while the module moves and the measuring wheel yaws to induce lateral creep. It records lateral and longitudinal forces and can determine the low creep curve in one pass, though this mode is unreliable. The TriboRailer and HO tribometer assess CoT in the low-creep regime, while hand-pushed tribometers operate in the high-creep regime.

Numerous studies have shown that contact pressure affects CoT assessment [81,82,86,87]. Higher contact pressure reduces the measured CoT, with the reduction slope depending on the wheel geometry and the third body layer. The scale factor also plays a role [33]. In addition to geometry and applied load, the state of the measuring wheel surface influences the CoT as the wheel wears in during measurements [88]. Most of the third body layer remains on the rail, so wheel cleaning slightly reduces the CoT. However, after a few passes, the CoT returns to its pre-cleaning value.

3.4 Knowledge Gap

The literature review revealed that the most frequently evaluated parameters for assessing the performance of TOR products are CoF/CoT, creep curve, carry distance and retentivity. However, comparing results across different studies is challenging, and sometimes even impossible, because many studies use non-commercial devices and experiments vary in terms of procedure, TORP application method, contact bodies and contact conditions. All of these differences affect the results. A similar maybe worse situation is in field trials. Short-term experiments utilizing portable devices are on the one side, whereas long-term trials performed under the operation are on the other side. Moreover, differences between tracks, weather conditions and third body layer affect the results. Nevertheless, most field studies confirm the TORP benefits investigated in the laboratory, but there is no approach ensuring the direct transferability of results from the laboratory to the field, e.g. the effect of TORP amount on the retentivity, carry distance etc. Is the dependency the same? This indicates the need for a unified testing methodology for the design and performance assessment of TORPs in laboratory settings. Moreover, the methodology should be able to assess the performance in conditions closer to reality. which would provide a connection between the laboratory and the field.

Assessing friction properties on the rail head is challenging due to the time-consuming and costly measurements required by instrumented trains, the complexity of using rail tribometers, and the low representativeness of simple portable devices like the Pendulum and the FricWear tribometer. Portable tribometers with rolling-sliding contact seem to be suitable alternatives. However, the commercial hand-pushed tribometer, which induces creep by braking the wheel, cannot assess the creep curve and requires tens of meters to measure CoT. This makes it nearly impossible to use in the laboratory or to investigate CoT

evolution on the same contact path after multiple passes. In contrast, the HO tribometer, which is mounted on the rail, can address these issues. It induces creep by steering the wheel, which may be considered less representative. Although adjusting the AoA allows the creep curve to be evaluated in one pass, this mode is unreliable. This highlights the need for a device that can assess the creep curve in a single pass and investigate CoT evolution on the same contact path in both the laboratory and the field.

4 AIMS OF THE THESIS

The main objective of this thesis is to develop a multi-phase methodology for evaluating the performance of TOR products, see Fig. 44. Each phase utilises different levels of simplification and aims at the assessment of various performance parameters. The first phase provides a universal tool comparing TORPs in terms of retentivity and risk of low adhesion, which can be used across laboratories. The second phase aims at the assessment of the track performance parameters (retentivity and the carry distance) under conditions closer to the actual wheel/rail contact. All mentioned parameters are determined based on the CoT. The third phase investigates the evolution of CoT in the field and correlates it with curve squeal. To achieve the main objective, I have to complete the following tasks:

T1 – propose a "standardized test" (further called Lab-to-Lab) enabling the evaluation of frictional properties of TOR products in the laboratory,

- **T1.1** – select a commercial tribometer providing sufficient wheel/rail representation, and determine the appropriate type of test,
- **T1.2** – define traction zones and parameters used in the performance evaluation,
- **T1.3** – verify the methodology on several TORPs,

T2 – develop the methodology (further called Lab-to-Field) evaluating track performance parameters in configuration closer to the actual wheel/rail contact

- **T2.1** – develop a portable rail tribometer allowing to assessment of CoT and creep curve shape on the actual rail,
- **T2.2** – design of tribometer's data processing and evaluation, and procedure to fit creep curves,
- **T2.3** – development of a contact simulator able to create a representative layer of TORP, which is similar to those in the field,
- **T2.4** – conduct the tests for the same TOPRs as in T1.3 and compare the results,

T3 – investigate the daily evolution of CoT in the field considering weather conditions,

T4 – correlate CoT with curve squeal observed in the field.

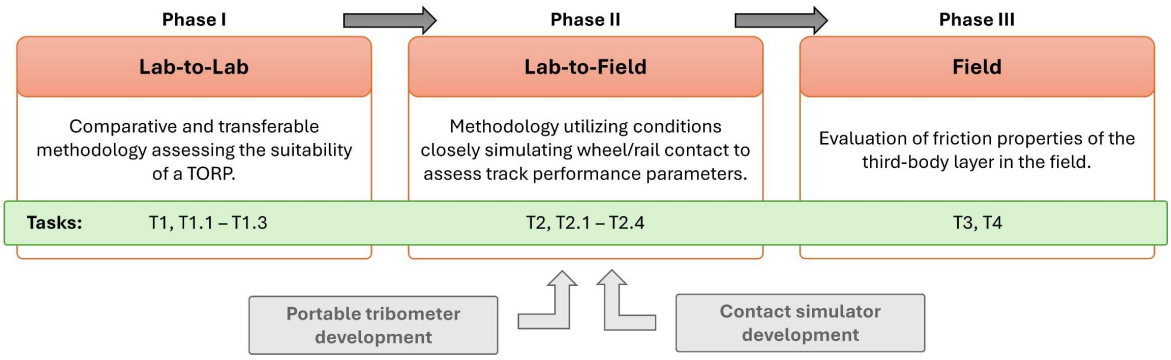

Fig. 44 The aim of the thesis

4.1 Methodology and Portable Rail Tribometer Requirements

Lab-to-Lab methodology requirements:

R1.1 – transferable – can be performed across different laboratories,
R1.2 – comparative results – performance classes Q1 - Q4,
R1.3 – representative results – cover a wide range of contact conditions,
R1.4 – good repeatability,
R1.5 – determine the effect of TOR products amount,
R1.6 – multi-parameter evaluation,
R1.7 – definition of traction zones,
R1.8 – identify the suitable product for further testing.

Lab-to-Field methodology requirements:

R2.1 – evaluation of track performance parameters (carry distance and retentivity),
R2.2 – configuration closer to actual wheel/rail contact,
R2.3 – representative TORP layer,
R2.4 – determine the effect of TOR products amount,
R2.5 – evaluation of application strategy
R2.6 – multi-parameter evaluation,
R2.7 – determination of transfer mechanism.

Portable rail tribometer requirements:

R3.1 – traction regime – the braking torque induces a creep into the contact,
R3.2 – change of contact path,
R3.3 – repeatable pass in one contact path,
R3.4 – measurements in both directions,
R3.5 – change of measurement length,
R3.6 – different measuring modes – a small spot of TORP requires a different measurement approach than a longer continuous layer in terms of braking torque,
R3.7 – adjustable contact pressure,
R3.8 – measurements in the field,
R3.9 – immediate visualization of recorded data,
R3.10 – user-friendly evaluation procedure,
R3.11 – estimation of uncertainties of the measurement.

4.2 Scientific Questions and Hypotheses

Q1: *Will applying TORP lead to a critically low traction coefficient on the rail, as observed in the laboratory?*

H1: *In MTM and twin-disc devices, the CoT drops because the lubricant thickness in the contact path exceeds the size of the surface irregularities. However, in a configuration closer to the actual wheel/rail contact, more of the lubricant is displaced and spread over a larger area, resulting in a lubricant thickness that is less than the size of the surface roughness, therefore the CoT is not critically low.*

Many previous laboratory studies showed a significant drop in CoT immediately after applying TORL or FM [39,40,61,69,70]. This drop is caused by the larger amount of TORP relative to the contact area. The TORP is squeezed out of the contact, but enough remains to create a film thickness that exceeds the height of the asperities. Additionally, the TORP adheres to both specimens representing the wheel and rail, and due to the rotating motion, the spots with a portion of TORP come into contact again, increasing the amount in the contact area. In contrast, in the field, higher contact pressure causes more TORP to be squeezed out, as demonstrated in [64], spreading it over a longer area. Furthermore, around 50% of the TORP adheres to the wheel and is transferred to another location, creating a new contact area. This results in a lower overall film thickness.

Q2: *How does the performance of FM change with varying amounts and after the water dries?*

H2: *Higher amounts of FM will result in longer retentivity, maintaining the CoT above the critically low value. After drying, retentivity will be shorter, but the CoT will remain above the critically low threshold.*

The study [40] showed that higher amounts of wet complex FM provide a stable CoT for a longer time before it starts rising. However, another substance exhibited a different behaviour. After an initial rise, the CoT again dropped to the value observed immediately after application, though a higher amount still delayed the initial rise. Based on these observations, it can be hypothesised that a higher amount of wet FM will result in longer retentivity. In the case of dry FM, the same study indicated that the changes in CoT due to the amount applied are insignificant compared to the wet state. All amounts provided the same initial CoT, which was higher than that in the wet state. In contrast, another study [68] found that dry FM resulted in lower CoT than wet FM. Furthermore, higher amounts of FM in the dry state reduced the CoT, with some measurements showing CoT values below 0.05, a level considered critically low. This discrepancy may be attributed to differences in the testing devices used, namely the MTM and the torsion rheometer, as well as the thick FM layer preventing the contact of asperities on the specimens. Additionally, a weak interface between the specimen and the FM layer may contribute to the low CoT.

Q3: *How does the CoT change with varying RH and temperature throughout the day in the field?*

H3: *Higher RH and lower temperature in the morning will lead to a lower CoT, which will increase throughout the day as the RH decreases and temperature increases.*

Studies performed in the laboratory [55,56] showed a decreasing trend of CoT with rising RH while the slope depends on the temperature. The lower temperature provides a larger CoT reduction with rising RH [56]. From another point of view, rising temperature increases the CoT when the RH is constant. A similar dependency on the RH was observed in the field [79], but a significant scatter of CoT was presented. The study utilized the Pendulum and was conducted in several places and on several non-consecutive days while not considering the daytime. It can be assumed that the third body layers were not the same, because they evolved in time and under different conditions [52]. Additionally, different third body layers provide different CoT [88].

Q4: *What is the relationship between the CoT and squeal noise on the selected tram line?*

H4: *Higher CoT leads to higher SPL.*

A numerical study [17] showed that a higher CoT reduces the effective damping ratio, with the reduction being more significant at lower frequencies. This reduction makes the wheel/track system more unstable, potentially generating a curve squeal even without the presence of negative friction. The mode coupling mechanism is responsible for generating the squeal noise. Another numerical study [16] observed that higher CoT results in a greater intensity of curve squeal noise, while the frequencies remain unaffected. Since SPL and noise intensity are similar parameters, the SPL is expected to follow the same trend. Both studies [16,17] identified a CoT threshold that must be exceeded for curve squeal to occur.

4.3 Thesis Layout

The thesis layout (Fig. 45) reflects the development of a methodology for evaluating the performance of TOR products. The methodology is divided into three phases according to a level of simplification, while each phase reflects some requirements and scientific questions. The thesis is composed of four research papers that undergo the peer review process and are published in journals with an impact factor.

Some of the requirements placed on the methodology are partially conflicting, therefore it was decided to develop a multi-phase methodology, the first phase Lab-to-Lab, the second phase Lab-to-Field and the third phase Field, while the first and second phases reflect the requirements. The Lab-to-Lab methodology (**Paper [I]**) was developed for a commercial tribometer (MTM) and provides comprehensive information about the TOR product which represents its performance. To achieve high repeatability, a robust evaluation method was needed. The first

phase provides a tool to select suitable lubricants, which can then be tested in the second phase or even in the field. The Lab-to-Field methodology (**Paper [III]**) focuses on determining performance parameters closer to those on a real track (carry distance and retentivity). A representative TOR product layer is created on a contact simulator and then measured using a portable tribometer. Both devices had to be developed. **Paper [II]** describes the BUT rail tribometer and the evaluation procedure, as it is a unique device. In addition to the effect of contact pressure and contaminants on the rail, three evaluation approaches were compared, two of which fit the data with an analytical and numerical model of the creep curve. The third phase (**Paper [IV]**) focuses on studying the evolution of friction properties of the third body layer formed on the rail in the field. This layer can significantly alter the CoT, making it essential to understand its behaviour under various weather conditions before assessing the performance of a TORP in the field. Additionally, the correlations between CoT and several noise parameters were determined, taking weather conditions into account.

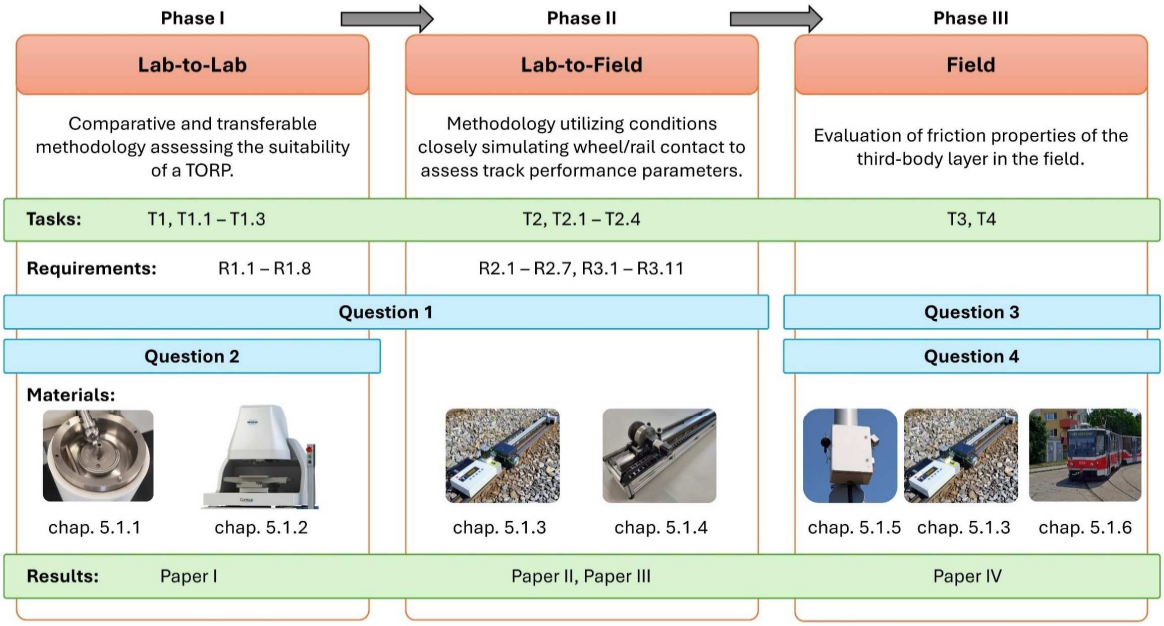

Fig. 45 General thesis layout

[I] GALAS R, SKURKA S, VALENA M, KVARDA D, OMASTA M, DING H, et al. A benchmarking methodology for top-of-rail products. Tribol Int 2023; 189: 108910. https://doi.org/10.1016/j.triboint.2023.108910.
IF = 6.1, AIS Quartile: Q1

(Author's contribution 20 %)

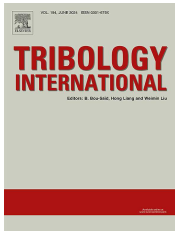

[II] VALENA M, OMASTA M, KVARDA D, GALAS R, KRUPKA I, HARTL M. An approach for the creep-curve assessment using a new rail tribometer. Tribol Int 2024; 191: 109153. https://doi.org/10.1016/j.triboint.2023.109153.
IF = 6.1, AIS Quartile: Q1*

(Author's contribution 60 %)

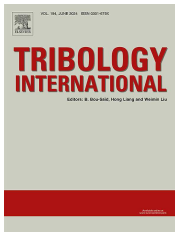

[III] GALAS R, VALENA M, JORDÁN T, KVARDA D, OMASTA M, SKURKA S, et al. A benchmarking methodology for top-of-rail products: carry distance and retentivity. Tribol Int 2024: 197: 109810. https://doi.org/10.1016/j.triboint.2024.109810.
IF = 6.1, AIS Quartile: Q1*

(Author's contribution 30 %)

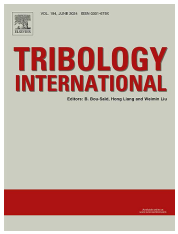

[IV] VALENA M, OMASTA M, KLAPKA M, GALAS R, NAVRATIL V, KRUPKA I, HARTL M. Case Study: Correlations Between Curve Squeal, Weather Conditions, and Traction in a Tram Loop. Tribology in Industry (manuscript)
Citescore = 2.8

(Author's contribution 65 %)

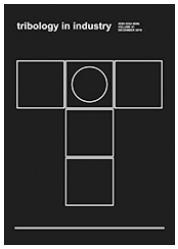

**Scientometric data for 2023 have been used as data for 2024 are not yet known.*

5 MATERIALS AND METHODS

5.1 Experimental Devices

As can be seen in Fig. 45, each phase needs different devices, some of them are commercial while others are custom-made and were developed at the Institute of Machine and Industrial Design. The first phase utilises MTM, for which a Lab-to-Lab methodology has been developed, and a profilometer to investigate the change in topography. The contact simulator and BUT rail tribometer had to be developed to achieve the requirements placed on the Lab-to-Field methodology. The experiments in the third phase were carried out in the field using the BUT rail tribometer and a noise module.

5.1.1 Mini Traction Machine

The MTM (Fig. 46) is a commercially available universal tribometer in a ball-and-disk configuration enabling standardized and special tests. The course of the test can be set or use predefined options, e.g. Stribeck curve measurement. The disk and 3/4-inch ball are driven separately, allowing the desired slip at contact to be set and maintained, which can range from -10,000 to +10,000%. One body rotates faster and the other slower while maintaining the set mean speed, which can be up to 4 m/s in either direction of rotation. The MTM can apply a normal force of up to 75 N (contact pressure of 1.25 GPa for standard samples), which is measured along with the traction force by a load cell. Standard specimens made of AISI 52100 bearing steel with initial roughness Ra=0.012 µm (ball) and Ra=0.01 µm (disc) were used. The device has a sampling rate of 1 Hz and the output is in .txt format. The file contains up to 14 variables of which time and traction coefficient are the most important.

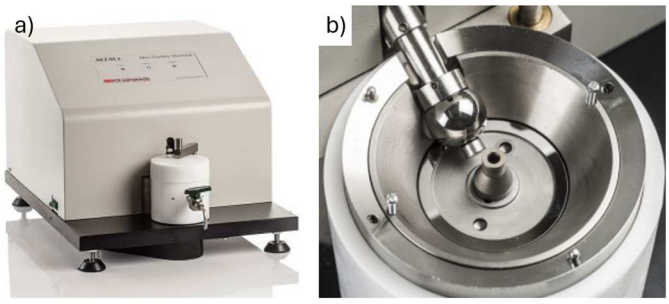

Fig. 46 a) Mini Traction machine, b)detail on specimens [89]

5.1.2 Profilometer

The Bruker Contour GT-X optical profilometer is used for non-contact measurement of surface topography and its subsequent evaluation. Two methods can be chosen for scanning.

The first is vertical scanning interferometry, which is suitable for rough surfaces and was used in this case. The scanning head moves towards the sample while recording the interference pattern, which also moves depending on the current distance of the surface from the scanning head. Subsequently, a 3D profile of the scanned surface is created. The second method is phase shifting interferometry, which is suitable for very smooth surfaces with a roughness of 0.01 μm or less.

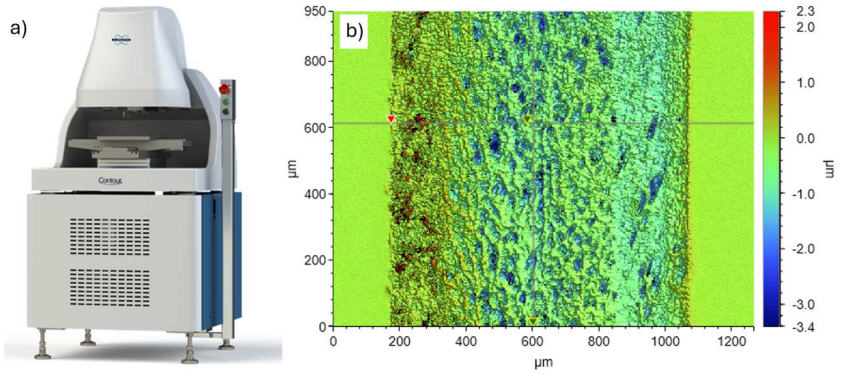

Fig. 47 a) Bruker Contour GT-X [90], b) contact path on the disc from MTM

The profilometer was used in the development of a lab-to-lab methodology to evaluate the groove width, groove depth and roughness on both contact bodies (ball, disc). Before the evaluation of these parameters, the surfaces were interleaved with a sphere in the case of a ball and with an inclined plane in the case of a disk. Furthermore, a Gaussian filter was applied to separate roughness and waviness. The evaluation was performed in Vision64 software from Bruker.

5.1.3 BUT Rail Tribometer

The BUT rail tribometer (Fig. 48) was developed as a part of this thesis. Its main advantage is that it can be operated in the field or the laboratory because it is powered by a power bank that can last a whole day of measurements, maybe even longer. The tribometer works in a traction regime that is more closely aligned with the conditions observed on a real track. The traction force in contact is induced by braking the measuring wheel while the slip is a consequence and depends on the frictional conditions in contact. The normal force is generated by the module weight and produces contact pressures of 0.8, 0.9 and 1 GPa depending on the number of weights. The BUT rail tribometer can operate in three different modes: constant, pulse and ramp.

The device comprises a horizontal linear unit with a carriage to which the measuring module is attached. On the sides of the linear unit are blocks with magnetic bases, through which the tribometer is fixed to the rail. The left block is equipped with a stepper motor that pulls the carriage with the measuring module, and the encoder is mounted on the right block. A wedge mechanism situated between the carriage and the measuring module enables the wheel

position to be altered between 0 and 8 mm. The measuring module comprises a measuring wheel attached to the encoder, brake and torque transducer.

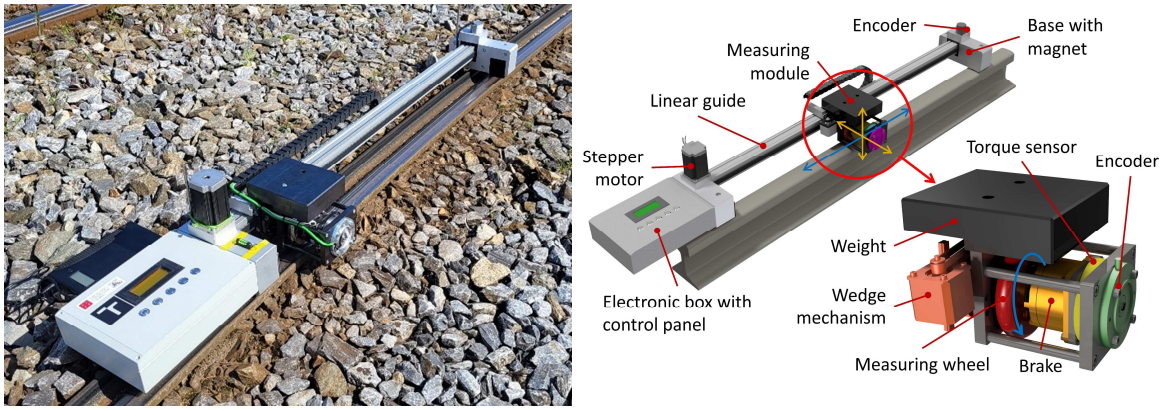

Fig. 48 BUT rail tribometer

During the measuring pass, the braking torque is controlled and simultaneously the torque sensor records it. In addition, the microcontroller records the time, longitudinal position of the measuring module and rotary position of the measuring wheel. The Gaussian filter is applied to a record of positions, from which the velocities are calculated. Creep is given by eq. (5) and pure sliding conditions correspond to 100%. The tangential force in the contact is obtained from an equilibrium of momentum, eq. (6). The normal force is not measured directly; it is assumed to be a constant that was determined from the actual mass of the measuring module and weights. The CoT is defined as the ratio of the tangential and the normal forces, see eq. (7). Detail information about BUT rail tribometer construction, measurement modes, data acquisition and their postprocessing can be found in **Paper [II]**.

$$creep = \frac{v_L - v_R}{v_L} \cdot 100\% \tag{5}$$

$$T = \frac{2}{D}(I\alpha + M_B) \tag{6}$$

$$CoT = \frac{T}{Q} \tag{7}$$

The tribometer is operated by five buttons and the set parameters and mode are displayed on the 4-line display. The left button starts the initialisation process. This must be done after switching on the tribometer. If the initialisation is not performed, the module might hit the right base. For such cases, the tribometer is equipped with a safety circuit that will cut off the power supply to the stepper motor, but it will not stop the measurement. The next button starts the measurement, the next is the enter key and the last two are used to scroll through the menu and change the parameters of the measurement mode or the mode itself. The tribometer can perform measurement passes without a laptop connected, but the data is not

stored anywhere. This feature may be used to run-in the rail or the wheel or, in general, where passes with controlled braking torque and varying creep are required.

As the BUT rail tribometer is equipped with custom-made electronics that record braking torque and positions from encoders, it was necessary to compare the outputs with the professional measuring card (NI USB-6001) that has sufficient sampling rate and accuracy. A noise was presented in both signals thus the filtration was performed. Afterwards, the torque acquired by the microcontroller was in good agreement with that measured via the NI card. A similar procedure was performed for encoders. The voltage change (pulses) was recorded by the microcontroller and NI card simultaneously. The tribometer evaluates pulses automatically, but the record from the NI card had to be postprocess. The difference was dependent on the set sampling rate in the tribometer, which affects the presented noise. It was decided to choose 10 Hz (the highest) and filter the position signal afterwards, therefore several filtering techniques were tested – moving average, exponential moving average, double exponential moving average and Gaussian filter. All techniques cause a delay in the speed change depending on the filter strength, which is unwanted as the circumferential speed changes rapidly when the wheel is blocked. A strong filter resulted in an artificial shift of the saturation point to higher creeps, but on the other hand, the velocity record was smoothed. Weak filters respond well to the change but do not remove the noise sufficiently. The Gaussian filter with a window size of 5 samples came out as the best from testing filters and their settings and is used further.

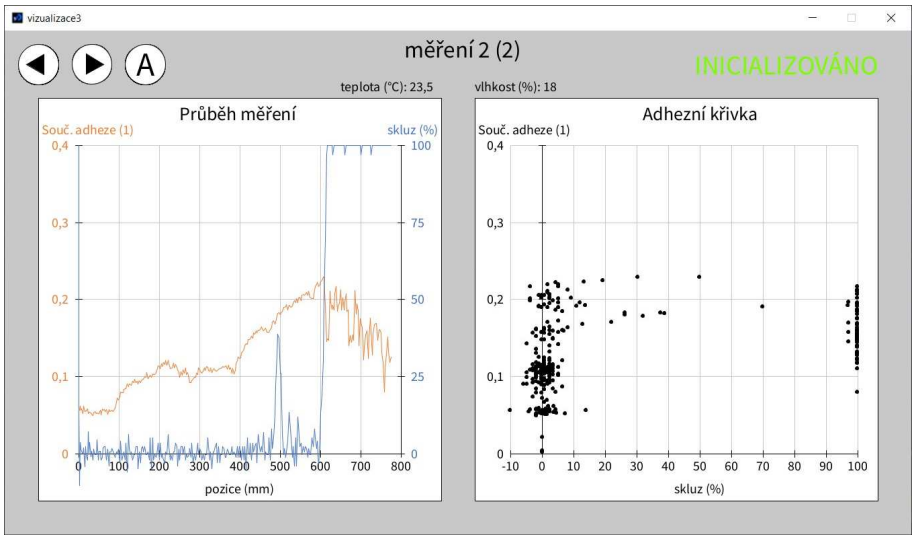

Fig. 49 Visualization program (labels in Czech)

In addition to the tribometer, several supporting files were created. The first is a data visualisation immediately after the measurement passes, showing creep and CoT as a function of position and creep curve, see Fig. 49. Both graphs are important for the subsequent adjustment of the pass parameters. The program allows you to scroll through the individual passes and plot the overall creep curve. It also automatically saves the raw data from all the measurements. It is therefore possible to perform a torque calibration after the

measurements have been taken. The next file is a Matlab script that processes the raw data and puts the result (module position, slip and CoT) into a pre-prepared Excel file. Several measurement files can be processed at once, but the maximum number of passes is 200. At this stage, it is necessary to have the final calibration constants that will be entered into the script. If the calibration constants are wrong, it is possible to repeat the procedure with the correct constants and create a new Excel file. The last file is the Excel file as mentioned above, which allows basic processing. It shows the creep and CoT as a function of position and creep curve for all runs. It also shows the total creep curve. It automatically evaluates effective CoT (CoT_e) and CoT_{max} from the selected area. The user can trim the data based on position, creep and CoT, which is important for evaluating friction conditions on a section of the track.

5.1.4 Contact Simulator

The contact simulator (Fig. 50) is another custom-made device designed at the Institute of Machine and Industrial Design. It represents the actual situation on the rail track as the wheel rolls on the rail, allowing the creation of a representative third body layer on the rail. This device serves only to create layers that are further investigated via BUT rail tribometer or other measuring devices. The contact simulator comprises interchangeable segments of the S49 rail, each measuring 1 m in length, and a cylindrical wheel made of bearing steel with a diameter of 150 mm. The wheel is connected to the stepper motor via a gearbox that controls the linear motion along the rail (0.2 m/s). The frame with the wheel and motor is mounted on a linear guide, ensuring movement and force transfer. The pinion is fixed at the end of the shaft and, in conjunction with the rack, induces a constant creep of 1.67% into contact between the cylindrical wheel and the rail segments. The contact pressure of 0.7 GPa is achieved by a lever on which the wheel is mounted and two bolts with coil springs. As the bolts are tightened, the springs are compressed and exert a force on the lever with the wheel against the rail.

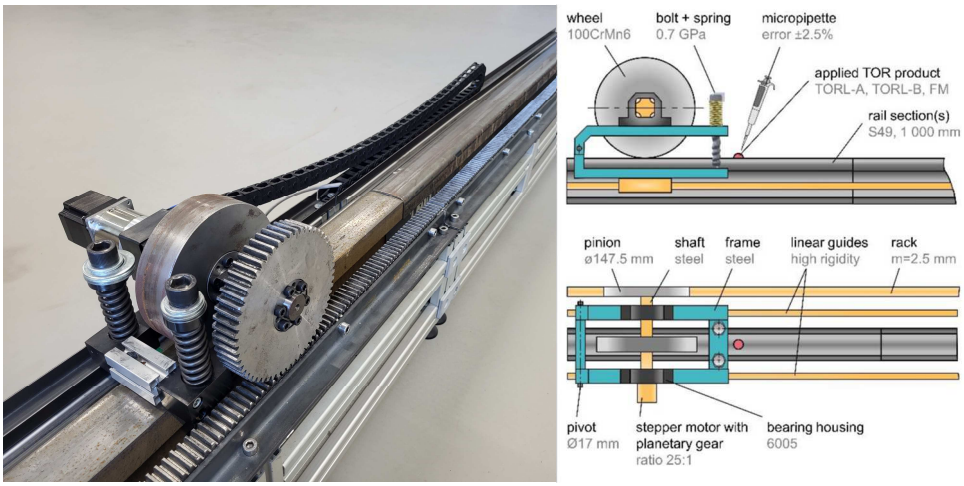

Fig. 50 The contact simulator

5.1.5 Noise Module

The noise module (Fig. 51) is the last custom-made device used in the dissertation thesis. It was designed at the Institute of Machine and Industrial Design in 2022. The main aim of the device is to automatically distinguish between squeal and flange noises and make records when a certain threshold is exceeded. The device consists of a programmable logic controller with a vibration measurement card to which is connected. The noise module is equipped with temperature, humidity, and rain sensors. it is powered by a battery that can last a week. The solar panel can also be used to charge the battery, allowing the noise module to operate for longer. The noise module performs real-time fast furrier transformation (FFT) analysis, which is used to distinguish between frequency bands characterising squeal and flange noise. The acoustic pressure is evaluated in the following frequency bands, derived from preliminary measurements, and can be adjusted to a specific location. It should be noted that the bands are narrow and may not contain pronounced frequencies, as they may alter due to differences in the rail system and tram.

- Squeal noise: 500 – 650 Hz,
- Flange noise: 3800 – 5800 Hz.

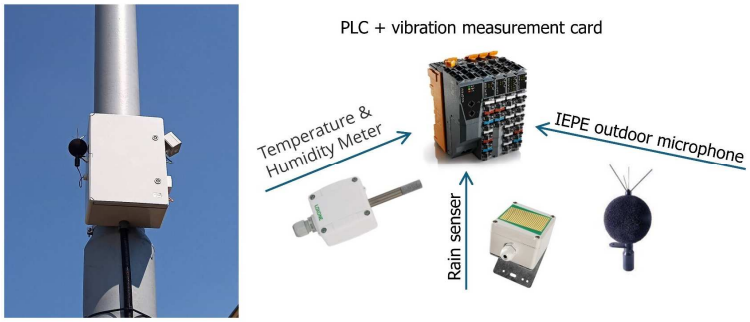

Fig. 51 Noise module

5.1.6 Field Measurements

The noise generated by trams was studied on a tram loop in the northwest part of Brno, Czechia, where the curve squeal occurred frequently and had a strong impact on the people living in the surrounding area. This resulted in numerous complaints connected with the noise produced by trams.

The tram loop in regular operation was selected, see Fig. 52. The entry curve with a radius of 21 m is placed in a road, which was not operated frequently. The rails in the rest of the loop are mounted on concrete sleepers that are completely covered with ballast. The tram stop is placed just after the exit of the curve. The tram line was operated by a single vehicle Tatra KT8D5 in a 15-minute interval, every day from 4:45 to 22:45 and the entering speed was limited to 15 km/s. The tram is bi-directional and consists of three body sections that

are connected by joints and thus can rotate each other in all directions. The body sections are mounted on four pivoting bogies (two internal and two external), each of which is fitted with two powered wheel sets.

Fig. 52 Tatra KT8D5 entering the tram loop

5.2 Methodology and experiment design

5.2.1 Phase I – Lab-to-Lab methodology

At this stage, the MTM was mainly used while the profilometer was utilized in the initial tests to check the surface topology of the contact bodies. All tests were carried out with a load of 18 N, which produces a contact pressure of 800 MPa, corresponding to light trains. The speed of 1 m/s was chosen because it is often used for tribological testing.

Two initial sets of tests were performed to determine the length of the wear-in and run-in procedures and to define a threshold curve and traction zones. The new test specimens were cleaned in an ultrasonic bath with a solvent for 20 minutes to remove any preservative oil. The first test set counted twenty 30-minute tests under dry conditions and an SRR of 2%. In addition to the CoT measured during the test, the roughness (Sq) and the width of the contact path were evaluated after each test. In the second set of tests, the SRR varied from 0 to 50% and lasted for 25 s. The CoT did not change significantly after 20% SRR, so only the interval from 0% to 20% was chosen. Based on the baseline obtained from the second test set and literature, the following traction zones were defined:

- retentivity traction zones: 0% – 66.7% of baseline
- intermediate traction zones: 33.3% – 66.7% of baseline
- low traction zones: 16.7% – 33.3% of baseline
- critical traction zones: 0% – 16.7% of baseline.

The Lab-to-Lab methodology consists of an experimental phase and an evaluation phase and counts nine steps in total, see Fig. 53, while the experimental phase can be further divided into a preparation phase and a measurement phase. The five consecutive performance tests are required to evaluate the performance of TORP, the first of which differs slightly from the others because the new pair is used. The first step is to clean the new or used pair in an ultrasonic bath with a solvent for 20 minutes. The next step depends on whether the pair is new or used. In the case of a new pair, the 60-minute wear-in is carried out mainly to stabilise the development of the path width, while also stabilising the roughness and the CoT, while in the case of a used pair, the 20-minute run-in is carried out to stabilise the roughness and the CoT. The TORP is then applied to the contact path on the disc using a micropipette and the total amount is divided into several equally distributed points with an amount of 1 µl. The fourth step is the traction test, which consists of six consecutive 30-sec sequences with gradually increasing SRR from 0% to 20%. This is followed by the check-point, where the CoT is checked to see whether or not it has exceeded the thresholds defined by the retentivity traction zone. Note that two consecutive points must meet this criterion. If the checkpoint is fulfilled, the next performance test can be carried out or the experimental phase can be stopped if it is the fifth performance test. Otherwise, the ball is cleaned with a dry paper towel and another traction test is carried out. This is repeated until the checkpoint is met.

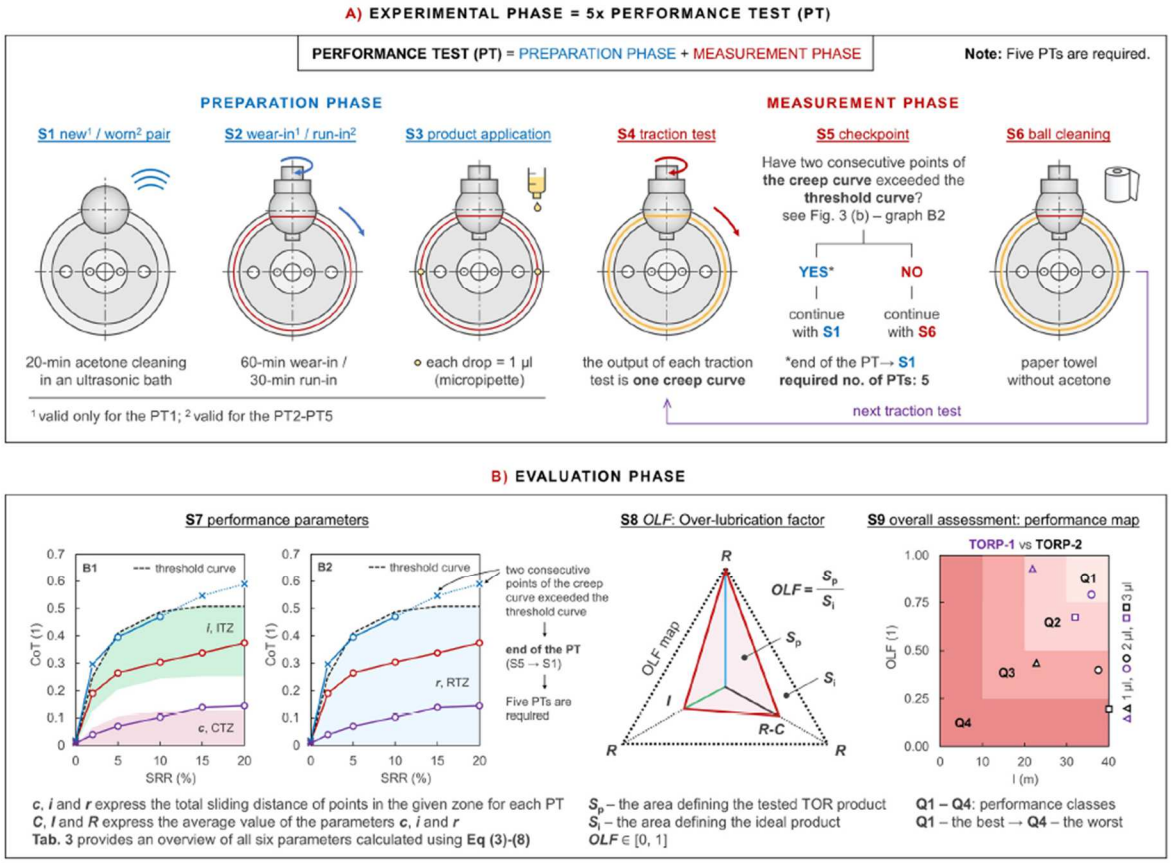

Fig. 53 Lab-to-lab methodology for assessing the performance of TORP

After five performance tests, the evaluation phase begins. First, the parameters *c*, *i* and *r* are calculated for each performance test and then averaged to give *C*, *I* and *R* respectively.

Parameters with lowercase letters indicate a total sliding distance in a particular traction zone of a single performance test, while those with uppercase letters indicate an average sliding distance over the performance tests. The over-lubrication factor (OLF) parameter is calculated from *C*, *I* and *R* and then the OLF map can be plotted. The OLF parameter ranges from 0 to 1, where 1 is the best result where over-lubrication cannot occur. The final step is to assign the performance class to the TORP with a certain amount applied. Further details can be found in the **Paper [I]**.

5.2.2 Phase II – Lab-to-Field Methodology

At this stage, several measurements were taken with the tribometer to verify it, establish the measurement procedure and understand its behaviour under different conditions. The first series of measurements covered common rail conditions, i.e. solvent cleaned, run-in, contaminated by water and by a TORP. All these measurements were made under contact pressures of 0.8, 0.9 and 1 GPa. Based on these measurements, a measurement procedure was established with the aim of making measurements with the lowest possible number of passes with pure creep. A further series of tests evaluated the repeatability of the measurements in terms of the resulting creep curves and the CoT_e. A conventional oil-based lubricant (WD-40) was applied to the rail, which ensured the same conditions throughout the test, while reducing CoT and consequently wear on both wheel and rail. A final series of tests were carried out in the laboratory and in the field to investigate the evolution of CoT. In the laboratory, the rail was cleaned and no run-in was performed. In the field, a visually clean section was selected and no run-in was performed, but the rail was cleaned in one case and not in another. Details can be found in the **Paper [II]**.

Further experiments (four test sets) were carried out on the contact simulator, while the BUT rail tribometer was used to evaluate the frictional properties of the created third body layers. As in the case of the Lab-to-Lab methodology, the first set of tests was carried out to investigate the run-in process with the wheel of the contact simulator at a contact pressure of 0.7 GPa. The wheel and rail were cleaned with solvent. The evolution of the CoT was recorded every 20 passes of the wheel of the contact simulator, for a total of 200 passes. Based on this, the length of the run-in process was defined and a further three traction zones were determined to enable the OLF calculation. Compared to the lab-to-lab method, the thresholds do not change over the creep, as the creep is a result of the set braking torque and frictional properties in the contact.

The following three sets of tests (sets no. 2-4) were carried out with TORP, investigating real performance parameters such as carry distance (how far the product spreads and is effective) and retentivity (how long the product is effective). Each of these series followed the run-in process, counting 120 passes. In the case of carry distance, the TORP was applied to the rail using a micropipette, the puddle was squeezed by a contact simulator wheel,

creating an imprint on the wheel which was then transferred to the rail. CoT was assessed on every 4th imprint. Retentivity was only assessed at the point of application. The contact simulator wheel made the pass over the imprint and was wiped off with a paper towel. This was repeated until the CoT did not exceed the threshold. As this is a time-demanding experiment, the imprint was analysed after a certain number of passes, specifically after 1, 10, 20, 30, 60, 100 and 150 passes. Test set 2 aimed to determine the optimum amount of TORP for subsequent testing, as an oil-based TOR lubricant may be dependent on the amount applied. Four different volumes were tested and 80 µl was identified as the most appropriate volume for further testing. Test set 3 investigated the carry distance, OLF and transfer behaviour of the best-performing TOR product by wiping the imprints on the rail with a paper towel which was then weighed. The test set 4 was designed to investigate the retentivity and creep curves. Three TORPs were used in set no. 3 and 4. Further details can be found in the **Paper [III]**.

5.2.3 Phase III – Field

This phase aims to evaluate the friction properties of the third-body layer formed in the field and to assess the correlation with the noise parameters measured by the noise module. For this purpose, the form of a case study was chosen.

The case study lasted several months during which the automatic noise module recorded three noise parameters and weather conditions. This was preceded by a one-day calibration measurement using the Class I sound level meter to identify the frequency bands of squeal and flange noise further used in the noise module. The main part of the study was carried out one day when the CoT was also measured using the BUT rail tribometer from 7:30 to 16:00. The CoT was evaluated on the left and right rail at three spots (30 m between them) approximately every hour, making a total of 48 measurements. The CoT was calculated using the median method in the creep interval from 5% to 15%, where the saturation point should occur. Details can be found in the **Paper [IV]**.

6 RESULTS AND DISCUSSION

The results of this thesis were published in four peer-reviewed **papers [I – IV]**, see Fig. 54. **Paper [I]** describes the Lab-to-Lab methodology aimed at ensuring the transferability and comparability of results using the MTM. This is the first step in evaluating TORP performance. **Paper [III]** outlines the Lab-to-Field methodology, the next step in the evaluation process, investigating more realistic parameters such as carry distance and retentivity under configuration closer to the actual wheel/rail contact. For this purpose, the BUT rail tribometer was developed to assess CoT and the creep curve on the actual rail, either in the laboratory or the field. **Paper [II]** provides a detailed description of the tribometer and the evaluation methods. The final **Paper [IV]** focuses on the evaluation of friction properties of the third-body layer affecting CoT and further noise generated by a tram.

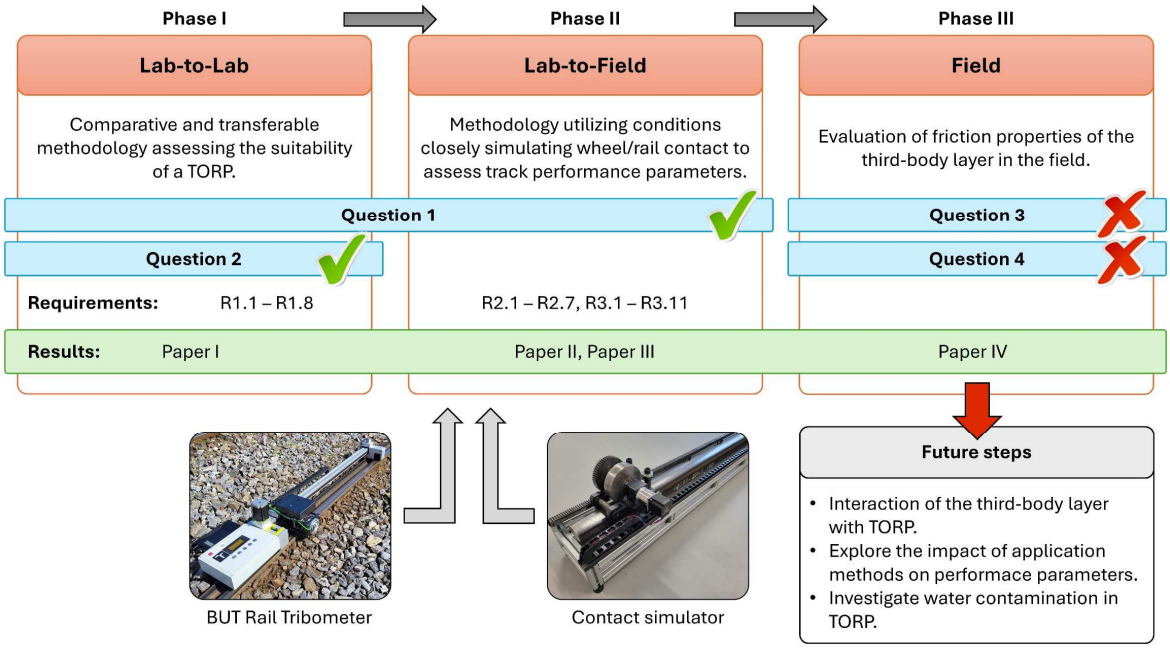

Fig. 54 Thesis results and further development

The Lab-to-Lab methodology presented in **Paper [I]** was tested on two TORLs, one FM, and one bleed oil. The results indicate that TORLs are more likely to cause low CoT than FM, and this risk increases with higher amounts. These findings align with previous studies, which observed lower CoT with higher TORL amounts [32,39,70] and better resistance to low CoT with FM [18]. The bleed oil achieved the lowest OLF while having similar effective retentivity to higher amounts of TORLs. Effective retentivity is more sensitive to the applied amount for TORLs compared to FM, suggesting that TORLs can provide longer retentivity. The retentivity of FM strongly depends on their state, whether they are dry or wet.

The standard CEN/TS 15427–2-2:2021 [63] was published during the development of the Lab-to-Lab methodology. Both methods utilise the MTM with specimens made of bearing

steel and perform a wear-in process before the main measurement. However, the experiment's course and the evaluation phase differ significantly. To evaluate TORP performance, the CEN/TS standard requires a single test assessing the creep curve and simple criteria, such as reaching the defined CoT level. In contrast, the Lab-to-Lab methodology covers a broader range of contact conditions by requiring five performance tests, each consisting of several traction tests. Additionally, it evaluates two parameters describing TORP behaviour and assigns the TORP to a performance class based on these parameters. The CEN/TS standard uses a prescribed TORP amount that is significantly higher than the amount tested in **Paper [I]** and does not account for its influence on performance. Conversely, the Lab-to-Lab methodology can test varying TORP amounts. The CEN/TS standard may be suitable for rapid testing of a larger number of TORPs.

The Lab-to-Field methodology presented in **Paper [III]** evaluates track performance parameters of TORP (carry distance, retentivity, transfer mechanisms and OLF) on the actual rail in the laboratory, which ensures stable conditions and suppresses the effect of the natural third body layer presented in the field. The methodology was tested on the same TORPs as the Lab-to-Lab methodology and not only on the best-performing TORP. The results show a strong correlation with Lab-to-Lab methodology in terms of retentivity and OLF while the TORL-B was identified as the best one. The methodology showed that a higher amount of TORL provides a longer carry distance, aligning with the findings of the study [45], which showed that the effect of the amount depends on the type of substance. Moreover, lower CoT was observed at the application point, which corresponds with many laboratory studies [32,39,70], but it is less severe than observed on small-scale tribometers. The FM exhibits a lower tendency to overlubricate the contact than TORLs, as the OLF factor is the highest. For TORLs, only the application point is critical because the OLF rapidly increases in the following imprints. TORLs provide longer retentivity and carry distance than FM.

The contact simulator was operated under 0.7 GPa of contact pressure which is slightly less than the typical pressure for light railway systems and notably lower than pressures for heavy haul systems. Higher contact pressure squeezes more TORL out of the contact path [64] and increases the consumption rate of TORP [65,66], therefore the actual retentivity and carry distance may be lower, but this fact is not important for the assessment of best-performing TORP. In the field, the phantom applicators have been observed. This means that a TORP was identified on the rail far away from the application point, but it was not detected in between. It is caused by TORP adhered on the wheel outside of the contact band, which re-enters the contact when the contact band is changed due to hunting on the tangent railway or a curve negotiation [64]. Another phenomenon causing phantom applicator is the TORP strings created between the wheel and the rail, which lend into the contact band [66]. These phenomena may prolong the carry distance [66], but in Lab-to-Field methodology are neglected.

Direct comparison of results obtained by BUT Rail Tribometer in **Paper [II]** to those from other portable tribometers is challenging due to varying friction properties of the measured third body layers, which significantly affect the CoT, and differences in the tribometers' kinematics, body sizes, and materials. Therefore, straightforward comparisons between tribometers can be misleading. The measurements performed under various contact conditions and contaminants confirmed the statement that higher contact pressure reduces the CoT, which was previously observed in studies [81,82,87,91]. It was shown that a solvent can degrade or break the third-body layer presented in the field because the CoT started to rise after the cleaning similarly as in the laboratory, while before the cleaning the CoT was stable throughout 20 passes. It should be noted that three evaluating procedures with different complexity were proposed but the resulting CoTs were nearly the same.

Paper [IV] was aimed at the evaluation of frictional properties of the third-body layer presented on the rail in the field. The frictional properties change concerning the weather conditions and daytime. In addition to CoT, the noise parameters like noise duration, SPL rms and max SPL were recorded by the noise module. It was shown that SPLs have a similar trend for varying temperatures and RH as previously observed for the sound power level [14]. However, noise duration showed a higher correlation with squeal noise and a slightly lower correlation with flange noise, indicating its suitability as a parameter for evaluating noise. Moreover, noise duration is independent of noise propagation, which varies with air humidity and precipitation. Additionally, noise duration exhibited the same trend as the probability of squeal [12]. The study revealed interesting correlations between CoT, weather conditions and squeal noise parameters, which will be discussed further in relationship to **Q3** and **Q4**.

6.1 Validation of Requirements

Several requirements (**R1.1 – R1.8**) were imposed on the Lab-to-Lab methodology (**Paper [I]**), all of which the proposed methodology meets. A universal tribometer (MTM) was chosen to ensure transferability and comparability of results, and product performance classes were introduced. Due to changing conditions during the test, a robust evaluation phase was necessary. This phase involves repeating the same test multiple times, thereby testing the product under varied conditions and making the results more representative.

The Lab-to-Field methodology (**Paper [III]**) meets most of the defined requirements (**R2.1 – R2.7**). The only requirement not experimentally verified is **R2.5**, which pertains to the evaluation of application strategies. However, based on the experiments conducted, it can be concluded that the methodology can also fulfil this requirement. To meet these requirements, two devices were developed. One of these devices is unique in its ability to measure CoT

under both laboratory and field conditions, ensuring comprehensive and reliable data collection across different environments.

The developed BUT Rail Tribometer (**Paper [II]**) combines the advantages of other tribometers. It operates under rolling-sliding conditions, inducing creep by braking the measuring wheel, similar to the Hand-pushed tribometer [81,82]. This approach is the most realistic besides using instrumented wheelsets or trains, as it simulates train braking. Additionally, the BUT rail tribometer is mounted on the rail like the HO tribometer [83], the Pendulum [77], and the FricWear [80], allowing for the investigation of local friction properties of the third body layer and its evolution in both laboratory and field conditions. From the other point of view, it might be a downside as the measured distance is limited. TriboMetro FR 101 [82], HO tribometer [83], and the BUT rail tribometer can all assess the entire creep curve. The TriboMetro FR 101 requires several meters of rail, which can distort results due to varying friction conditions along the measured section. The HO tribometer can evaluate the creep curve in a single pass, but this mode is unreliable. The BUT rail tribometer can also evaluate it in a single pass, but only if the measuring parameters are set appropriately. Evaluating the creep curve in a single pass is advantageous because it minimizes the negative effects of friction changes during repeated passes. The BUT rail tribometer has several downsides. Its construction and loading mechanism using weights allow measurement only on the top of the rail and not on the gauge side. This design also results in a higher device weight, although the measuring module can move vertically freely. Another downside is that the measuring wheel remains blocked when sufficient torque is developed and continues to the end of the pass, which may affect or damage the third body layer on the rail if it has low resistance. It can be concluded that the developed BUT Rail Tribometer meets all defined requirements (**R3.1 – R3.11**).

6.2 Scientific Questions and Hypotheses Validation

The following chapter addresses the scientific questions and hypotheses defined in Chapter 4.2 and provides an explanation for each hypothesis.

Q1: *Will applying TORP lead to a critically low traction coefficient on the rail, as observed in the laboratory?*

Hypothesis H1 was confirmed.

The question was addressed using the OLF parameter, which indicates the contact over-lubrication, and the CoT measured on the rail. **Paper [I]** demonstrated that OLF decreases with increasing amounts of TORL, while it remains constant for FM. Another key metric is the parameter c (slip distance in the critical traction zone), which is non-zero for TORLs. In contrast, **Paper [III]** revealed that the CoT at the application point

for small amounts of TORL-B is in the intermediate traction zone (CoT > 0.2). Although the amount of TORL-B was increased 20-fold (to 80 µl), the CoT was still above the critical traction zone. For other TORPs, the CoT was also above the critical traction zone. Notably, FM remained below the medium traction zone at the application point. As the number of imprints (carry distance) increased, both CoT and OLF also increased. For TORL, OLF values rose from 0.3 to 0.9 over the first four imprints, and for FM, values increased from 0.6 to 0.9. This suggests that traction issues are confined to the application site and its immediate vicinity.

Q2: *How does the performance of FM change with varying amounts and after the water dries?*

Hypothesis H2 was confirmed.

Based on the OLF parameter, which remains at a value of 1 in all cases, it can be concluded that FM does not cause a critically low CoT after drying, despite being tested with only one quantity. In publication [68], a small amount of dry FM resulted in a low CoT, whereas the same amount showed a negligible decrease in CoT before drying.

Given that OLF equals 1, retentivity can be assessed using the parameter I. **Paper [I]** demonstrated that as the amount of wet FM increases, retentivity also rises, nearly reaching the value for TORL, but only at 12 times the quantity. The reactivity of FM decreased by 75% after drying compared to the value measured in the wet condition.

Q3: *How does the CoT change with varying RH and temperature throughout the day in the field?*

Hypothesis H3 was falsified.

Paper [IV] revealed an increase in CoT with rising RH, which contrasts with laboratory studies [34,54–56,79]. A key difference is that laboratory studies are conducted under constant temperature, with water vapour added to an enclosed chamber to increase RH and simultaneously absolute humidity (AH). In the field study, however, AH remained almost constant, similar to the conditions in the study [54]. Another factor could be that the changes in RH were a response to temperature variation, as the field study was conducted on a sunny day.

Additionally, CoT was highest in the morning and gradually decreased throughout the day. The reference measurement, composed of readings taken first and last on another track, shows the same trend. Therefore, it can be concluded that changes in weather conditions play a major role in the variations of CoT observed in this case.

Q4: *What is the relationship between the CoT and curve squeal on the selected tram line?*

Hypothesis H4 was falsified.

The hypothesis had to be falsified even if it was partially correct.

The **Paper [IV]** observed a rising correlation between CoT and SPL rms, which was almost statistically significant according to the 95% confidence band. If only this parameter was evaluated, the hypothesis would be confirmed However, the maximum SPL was also recorded and did not show a correlation with CoT, suggesting it may not be an appropriate parameter for noise evaluation. On the other hand, the squeal noise duration reported a significantly higher correlation with CoT. The noise duration may be an appropriate parameter for evaluating the curve squeal because its value is independent of noise propagation in the environment which varies with air humidity and precipitations.

The content of pages 69-84 corresponds to ***Paper [I]***

https://doi.org/10.1016/j.triboint.2023.108910

Contents lists available at ScienceDirect

Tribology International

journal homepage: www.elsevier.com/locate/triboint

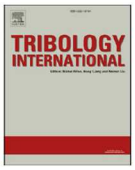

A benchmarking methodology for top-of-rail products

Radovan Galas [a,*], Simon Skurka [a], Martin Valena [a], Daniel Kvarda [a], Milan Omasta [a], Haohao Ding [b], Qiang Lin [b], Wen-jian Wang [b], Ivan Krupka [a], Martin Hartl [a]

[a] Faculty of Mechanical Engineering, Brno University of Technology, Technicka 2896/2, 616 69 Brno, Czech Republic
[b] Tribology Research Institute, State Key Laboratory of Traction Power, Southwest Jiaotong University, Chengdu 610031, China

The content of pages 85-94 corresponds to ***Paper [II]***

https://doi.org/10.1016/j.triboint.2023.109153

Contents lists available at ScienceDirect

Tribology International

journal homepage: www.elsevier.com/locate/triboint

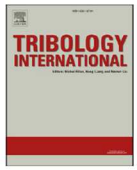

An approach for the creep-curve assessment using a new rail tribometer

Martin Valena *, Milan Omasta, Daniel Kvarda, Radovan Galas, Ivan Krupka, Martin Hartl

Faculty of Mechanical Engineering, Brno University of Technology, Technicka 2896/2, 616 69 Brno, Czech Republic

The content of pages 95-108 corresponds to ***Paper [III]***

https://doi.org/10.1016/j.triboint.2024.109810

Contents lists available at ScienceDirect

Tribology International

journal homepage: www.elsevier.com/locate/triboint

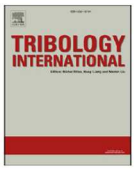

A benchmarking methodology for top-of-rail products: Carry distance and retentivity

Radovan Galas [a,*], Martin Valena [a], Tomas Jordan [a], Daniel Kvarda [a], Milan Omasta [a], Simon Skurka [a], Bingnan Wu [b], Haohao Ding [b], Wen-jian Wang [b], Ivan Krupka [a], Martin Hartl [a]

[a] Faculty of Mechanical Engineering, Brno University of Technology, Technicka 2896/2, 616 69 Brno, Czech Republic
[b] Tribology Research Institute, State Key Laboratory of Traction Power,Southwest Jiaotong University, Chengdu 610031, China

The content of pages 109-120 corresponds to ***Paper [IV]***
(manuscript)

Vol. xx, No. x (202x) x-x

Tribology in Industry

www.tribology.rs

RESEARCH

Case Study: Correlations Between Curve Squeal, Weather Conditions, and Traction in a Tram Loop

Martin Valena [a,*], Milan Omasta [a], Milan Klapka [a], Radovan Galas [a], Vaclav Navratil [a], Ivan Krupka [a], Martin Hartl [a]

[a] *Faculty of Mechanical Engineering, Brno University of Technology, Technicka 2896/2, 616 69 Brno, Czechia.*

7 CONCLUSIONS AND RECOMMENDATIONS

7.1 Conclusions

This dissertation focuses on the development of a multi-phase methodology for determining the performance of TORPs. A portable rail tribometer, crucial to this methodology, was also developed. This methodology is divided into three phases while each utilizes a different level of simplification.

The first phase utilises a universal tribometer and a robust evaluation procedure ensuring consistency and comparability of results across different laboratories. This phase aims to identify the best-performing TORP for further, more realistic tests and its susceptibility to the applied quantity. For this purpose, a comparative test with four classes was developed. The methodology phase provides an approach for the investigation of TORP behaviour, which can streamline and simplify the new product development process and reduce the number of various products tested under more realistic conditions.

The second phase determines the track performance parameters like retentivity and carry distance in the laboratory under configuration closer to actual wheel/rail contact. It provides an intermediate step between the field and the laboratory experiment as this phase assesses the performance of the representative TORP layers considering actual transfer mechanisms and suppressing the effect of the natural third-body layer. This methodology phase may reduce the number of field tests and optimize TORP application strategies, including the distance between wayside units and the timing between dosages.

The third phase focuses on the evolution of friction properties of the third-body layer in the field, influenced by weather conditions and time of day. This step was essential before assessing TORP performance in the field, as the actual third-body layer can significantly impact performance. Additionally, An automatic noise module capable of distinguishing between squeal and flange noise was employed to monitor SPL rms, maximum SPL, and noise duration. It provides valuable insight into the evolution of CoT and noise parameters during the day.

The developed BUT rail tribometer is a unique device that enables the determination of the CoT and the shape of the creep curve on the rail both in the laboratory and in the field. The tribometer's greatest advantage is its ability to determine the creep curve within a single pass, given the correct parameter settings, and to perform repeated passes on the same contact track. This capability allows for the investigation of the third-body layer resistance and the comparison of laboratory and field results, providing valuable insights into the formation of friction layers on the track. Additionally, the tribometer can determine CoT locally, which was used for evaluating track performance parameters within the developed methodology.

The main findings of this thesis can be summarised in the following points:

- The methodology pointed out that TORLs are more likely to produce low CoT compared to FM. However, the drop in CoT is less severe on actual rails than in small-scale tribometers.
- TORLs exhibit longer retentivity and carry distance than FM. While CoT at the application point is initially lower and it rapidly increases with distance from the application point.
- TORL puddles distribute between the rail and the wheel in a 45:55 ratio, with 44% of the TORL on the wheel remaining on the sides of the contact band and not re-entering it during experiments.
- A significant correlation was observed between CoT and the duration of squeal noise, whereas the association with SPL was less pronounced. The duration of noise appears to be a suitable parameter for noise evaluation, as it remains unaffected by environmental factors like air humidity and precipitation.

7.2 Future Steps and Recommendations

Based on the presented multi-phase methodology, the logical following step is field experiments. It is important to note that these experiments should not replicate the Lab-to-Field methodology experiments, except potentially one set used to validate the proposed approach. Field experiments are both costly and time-consuming, so their focus should be strategically chosen. The focus should be on investigating the interaction between TORPs and the third-body layer. As was demonstrated the CoT fluctuates with the time of day and varying weather conditions. Additionally, the combination of TORPs with the third-body layer can significantly influence performance parameters, particularly CoT.

The significance of this interaction is underscored by the study [35] conducted on an MTM, which revealed that even a small amount of water mixed with TORL can lead to a drastically reduced CoT. This finding indicates the necessity of studying this phenomenon in a configuration closer to actual wheel/rail contact.

As previously mentioned, the Lab-to-Field methodology should be capable of testing different application methods. However, this has not yet been verified experimentally. A potential next step is to investigate different application strategies that could preserve carry distance and retention while reducing the risk of overfitting. One such strategy could be to apply TORP directly to the wheel.

8 LIST OF PUBLI□ATIONS & OUT□OMES

8.1 Papers Related to the Thesis Topic

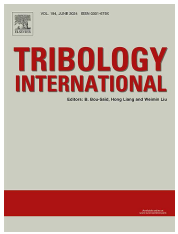

GALAS R, SKURKA S, VALENA M, KVARDA D, OMASTA M, DING H, et al. A benchmarking methodology for top-of-rail products. Tribol Int 2023; 189: 108910. https://doi.org/10.1016/j.triboint.2023.108910.
[IF = 6.1]

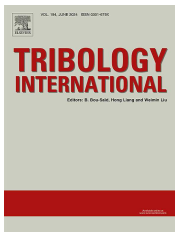

VALENA M, OMASTA M, KVARDA D, GALAS R, KRUPKA I, HARTL M. An approach for the creep-curve assessment using a new rail tribometer. Tribol Int 2024; 191: 109153. https://doi.org/10.1016/j.triboint.2023.109153.
[IF = 6.1]

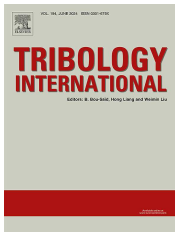

GALAS R, VALENA M, JORDÁN T, KVARDA D, OMASTA M, SKURKA S, et al. A benchmarking methodology for top-of-rail products: carry distance and retentivity. Tribol Int 2024: 197: 109810. https://doi.org/10.1016/j.triboint.2024.109810.
[IF = 6.1]

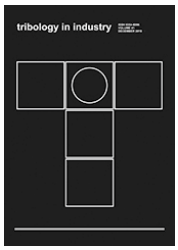

VALENA M, OMASTA M, KLAPKA M, GALAS R, NAVRATIL V, KRUPKA I, HARTL M. Case Study: Correlations Between Curve Squeal, Weather Conditions, and Traction in a Tram Loop. Tribology in Industry (manuscript)
[Citescore = 2.8]

8.2 Other Papers

ČERNÁK M, MICHALEC M, VALENA M, RANUŠA M. Inlet shape optimization of pneumobile engine pneumatic cylinder using CFD analysis. J Phys Conf Ser 2021; 1935: 012011. https://doi.org/10.1088/1742-6596/1935/1/012011.
[Citescore = 0.7]

8.3 Papers in Conference Proceedings

VALENA M. OMASTA M, HARTL M. Influence of weather conditions on the noise and the traction coefficient in curves with a small radius. Current problems in rail vehicles - PRORAIL 2023. https://doi.org/10.26552/spkv.Z.2023.2.43

VALENA M, OMASTA M, GALAS R, HARTL M. Development of a tribometer for evaluating adhesion on a real rail. Current Problems in Rail Vehicles 2021.

8.4 Functional Samples

OMASTA M, VALENA M, VODEHNAL M, VAŠÍČEK M. Field Tribometer for Assessment of Adhesion on the Rail. (Classified report)

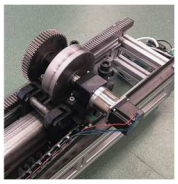

OMASTA M, GALAS R, KVARDA D, VALENA M, VAŠÍČEK M. Contact simulator; Contact simulator for creating friction layers on a rail. http://intranet.ustavkonstruovani.cz/file-download/get-project-pdf/438

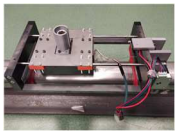

JORDÁN T, GALAS R, KVARDA D, VALENA M, OMASTA M, VAŠÍČEK M. Tribometer; Tribometer for measurement of shear friction on a rail. http://intranet.ustavkonstruovani.cz/file-download/get-project-pdf/439

8.5 Other Outcomes

VALENA M, GALAS R, OMASTA M, KŘUPKA I, HARTL M. Methodology for Assessing the Performance of Top-of-rail Products on Rail. Leeds-Lion Symposium on tribology, Leeds, UK, 2023 [Poster presentation]

9 LITERATURE

[1] Carter FW. On the action of a locomotive driving wheel. Proc R Soc London Ser A, Contain Pap a Math Phys Character 1926;112:151–7. https://doi.org/10.1098/rspa.1926.0100.

[2] Haines DJ, Ollerton E. Contact Stress Distributions on Elliptical Contact Surfaces Subjected to Radial and Tangential Forces. Proc Inst Mech Eng 1963;177:95–114. https://doi.org/10.1243/PIME_PROC_1963_177_014_02.

[3] Galas R. Friction Modification within Wheel-Rail Contact. Brno University of Technology, 2017.

[4] Lewis R, Olofsson U. Wheel-rail interface handbook. 1st pub. Cambridge: Boca Raton: Woodhead ; CRC Press; 2009.

[5] Grassie SL. Rail corrugation: Characteristics, causes, and treatments. Proc Inst Mech Eng Part F J Rail Rapid Transit 2009;223:581–96. https://doi.org/10.1243/09544097JRRT264.

[6] Thompson D. Railway Noise and Vibration. Elsevier; 2009. https://doi.org/10.1016/B978-0-08-045147-3.X0023-0.

[7] Remington PJ. Wheel/rail squeal and impact noise: What do we know? What don't we know? Where do we go from here? J Sound Vib 1987;116:339–53. https://doi.org/10.1016/S0022-460X(87)81306-8.

[8] Eadie DT, Santoro M, Kalousek J. Railway noise and the effect of top of rail liquid friction modifiers: changes in sound and vibration spectral distributions in curves. Wear 2005;258:1148–55. https://doi.org/10.1016/j.wear.2004.03.061.

[9] Hsu SS, Huang Z, Iwnicki SD, Thompson DJ, Jones CJC, Xie G, et al. Experimental and theoretical investigation of railway wheel squeal. Proc Inst Mech Eng Part F J Rail Rapid Transit 2007;221:59–73. https://doi.org/10.1243/0954409JRRT85.

[10] Fourie DJ, Gräbe PJ, Heyns PS, Fröhling RD. Frequency domain model for railway wheel squeal resulting from unsteady longitudinal creepage. J Sound Vib 2019;445:228–46. https://doi.org/10.1016/j.jsv.2018.12.014.

[11] Meehan PA. Investigation of chaotic instabilities in railway wheel squeal. Nonlinear Dyn 2020;100:159–72. https://doi.org/10.1007/s11071-020-05493-x.

[12] Liu X, Meehan PA. Investigation of the effect of relative humidity on lateral force in rolling contact and curve squeal. Wear 2014;310:12–9. https://doi.org/10.1016/j.wear.2013.11.045.

[13] Yang Z, Li Z. Numerical modeling of wheel-rail squeal-exciting contact. Int J Mech Sci 2019;153–154:490–9. https://doi.org/10.1016/j.ijmecsci.2019.02.012.

[14] Maly T, Biebl F, Ostermann M. The effects of weather conditions and wheel wear on curve squeal. Proc Int Congr Acoust 2019:1559–66.

[15] Liu X, Meehan PA. Investigation of squeal noise under positive friction characteristics condition provided by friction modifiers. J Sound Vib 2016;371:393–405. https://doi.org/10.1016/j.jsv.2016.02.028.

[16] WANG J. Influence of Friction Coefficient on Wheel-rail Curve Squeal Noise. J

Mech Eng 2018;54:255. https://doi.org/10.3901/JME.2018.04.255.

[17] Feng X, Chen G, Song Q, Dong B, Ren W. A Root Cause of Curve Squeal: Self-Excited Frictional Vibration of a Wheelset–Track System. J Tribol 2024;146:1–20. https://doi.org/10.1115/1.4064509.

[18] Stock R, Stanlake L, Hardwick C, Yu M, Eadie D, Lewis R. Material concepts for top of rail friction management – Classification, characterisation and application. Wear 2016;366–367:225–32. https://doi.org/10.1016/j.wear.2016.05.028.

[19] Harmon M, Lewis R. Review of top of rail friction modifier tribology. Tribol - Mater Surfaces Interfaces 2016;10:150–62. https://doi.org/10.1080/17515831.2016.1216265.

[20] Kalousek J, Johnson KL. An Investigation of Short Pitch Wheel and Rail Corrugations on the Vancouver Mass Transit System. Proc Inst Mech Eng Part F J Rail Rapid Transit 1992;206:127–35. https://doi.org/10.1243/PIME_PROC_1992_206_226_02.

[21] Suda Y, Iwasa T, Komine H, Tomeoka M, Nakazawa H, Matsumoto K, et al. Development of onboard friction control. Wear 2005;258:1109–14. https://doi.org/10.1016/j.wear.2004.03.059.

[22] Aldajah S, Ajayi OO, Fenske GR, Kumar S. Investigation of Top of Rail Lubrication and Laser Glazing for Improved Railroad Energy Efficiency. J Tribol 2003;125:643–8. https://doi.org/10.1115/1.1537745.

[23] Matsumoto A, Sato Y, Ohno H, Tomeoka M, Matsumoto K, Ogino T, et al. Improvement of bogie curving performance by using friction modifier to rail/wheel interface. Wear 2005;258:1201–8. https://doi.org/10.1016/j.wear.2004.03.063.

[24] MATSUMOTO K, SUDA Y, IWASA T, FUJII T, TOMEOKA M, TANIMOTO M, et al. A Method to Apply Friction Modifier in Railway System. JSME Int J Ser C 2004;47:482–7. https://doi.org/10.1299/jsmec.47.482.

[25] VanderMarel J, Eadie DT, Oldknow KD, Iwnicki S. A predictive model of energy savings from top of rail friction control. Wear 2014;314:155–61. https://doi.org/10.1016/j.wear.2013.11.037.

[26] Seo JW, Jun HK, Kwon SJ, Lee DH. Effect of Friction Modifier on Rolling Contact Fatigue and Wear of Wheel and Rail Materials. Tribol Trans 2018;61:19–30. https://doi.org/10.1080/10402004.2016.1271487.

[27] Eadie DT, Elvidge D, Oldknow K, Stock R, Pointner P, Kalousek J, et al. The effects of top of rail friction modifier on wear and rolling contact fatigue: Full-scale rail–wheel test rig evaluation, analysis and modelling. Wear 2008;265:1222–30. https://doi.org/10.1016/j.wear.2008.02.029.

[28] Eadie DT, Santoro M, Oldknow K, Oka Y. Field studies of the effect of friction modifiers on short pitch corrugation generation in curves. Wear 2008;265:1212–21. https://doi.org/10.1016/j.wear.2008.02.028.

[29] Eadie DT, Santoro M. Top-of-rail friction control for curve noise mitigation and corrugation rate reduction. J Sound Vib 2006;293:747–57. https://doi.org/10.1016/j.jsv.2005.12.007.

[30] Egana JI, Vinolas J, Gil-Negrete N. Effect of liquid high positive friction (HPF) modifier on wheel-rail contact and rail corrugation. Tribol Int 2005;38:769–74.

https://doi.org/10.1016/j.triboint.2004.11.006.

[31] Eadie DT, Santoro M, Powell W. Local control of noise and vibration with KELTRACK™ friction modifier and Protector® trackside application: an integrated solution. J Sound Vib 2003;267:761–72. https://doi.org/10.1016/S0022-460X(03)00739-9.

[32] Galas R, Omasta M, Klapka M, Kaewunruen S, Krupka I, Hartl M. Case Study: the Influence of Oil-based Friction Modifier Quantity on Tram Braking Distance and Noise. Tribol Ind 2017;39:198–206. https://doi.org/10.24874/ti.2017.39.02.06.

[33] Lundberg J, Rantatalo M, Wanhainen C, Casselgren J. Measurements of friction coefficients between rails lubricated with a friction modifier and the wheels of an IORE locomotive during real working conditions. Wear 2015;324–325:109–17. https://doi.org/10.1016/j.wear.2014.12.002.

[34] Lewis SR, Lewis R, Olofsson U, Eadie DT, Cotter J, Lu X. Effect of humidity, temperature and railhead contamination on the performance of friction modifiers: Pin-on-disk study. Proc Inst Mech Eng Part F J Rail Rapid Transit 2013;227:115–27. https://doi.org/10.1177/0954409712452239.

[35] Skurka S, Galas R, Omasta M, Wu B, Ding H, Wang W-J, et al. The performance of top-of-rail products under water contamination. Tribol Int 2023;188:108872. https://doi.org/10.1016/j.triboint.2023.108872.

[36] Abbasi S, Olofsson U, Zhu Y, Sellgren U. Pin-on-disc study of the effects of railway friction modifiers on airborne wear particles from wheel–rail contacts. Tribol Int 2013;60:136–9. https://doi.org/10.1016/j.triboint.2012.11.013.

[37] Sundh J, Olofsson U, Sundvall K. Seizure and wear rate testing of wheel–rail contacts under lubricated conditions using pin-on-disc methodology. Wear 2008;265:1425–30. https://doi.org/10.1016/j.wear.2008.03.025.

[38] Lu X, Cotter J, Eadie DT. Laboratory study of the tribological properties of friction modifier thin films for friction control at the wheel/rail interface. Wear 2005;259:1262–9. https://doi.org/10.1016/j.wear.2005.01.018.

[39] Galas R, Omasta M, Krupka I, Hartl M. Laboratory investigation of ability of oil-based friction modifiers to control adhesion at wheel-rail interface. Wear 2016;368–369:230–8. https://doi.org/10.1016/j.wear.2016.09.015.

[40] Galas R, Kvarda D, Omasta M, Krupka I, Hartl M. The role of constituents contained in water–based friction modifiers for top–of–rail application. Tribol Int 2018;117:87–97. https://doi.org/10.1016/j.triboint.2017.08.019.

[41] Cann PM. The “leaves on the line” problem - A study of leaf residue film formation and lubricity under laboratory test conditions. Tribol Lett 2006;24:151–8. https://doi.org/10.1007/s11249-006-9152-2.

[42] Lewis R, Gallardo EA, Cotter J, Eadie DT. The effect of friction modifiers on wheel/rail isolation. Wear 2011;271:71–7. https://doi.org/10.1016/j.wear.2010.10.036.

[43] Li Z, Arias-Cuevas O, Lewis R, Gallardo-Hernández EA. Rolling-sliding laboratory tests of friction modifiers in leaf contaminated wheel-rail contacts. Tribol Lett 2009;33:97–109. https://doi.org/10.1007/s11249-008-9393-3.

[44] Meierhofer A, Hardwick C, Lewis R, Six K, Dietmaier P. Third body layer-

experimental results and a model describing its influence on the traction coefficient. Wear 2014;314:148–54. https://doi.org/10.1016/j.wear.2013.11.040.

[45] Chen H, Fukagai S, Sone Y, Ban T, Namura A. Assessment of lubricant applied to wheel/rail interface in curves. Wear 2014;314:228–35. https://doi.org/10.1016/j.wear.2013.12.006.

[46] Matsumoto A, Sato Y, Ono H, Wang Y, Yamamoto M, Tanimoto M, et al. Creep force characteristics between rail and wheel on scaled model. Wear 2002;253:199–203. https://doi.org/10.1016/S0043-1648(02)00100-X.

[47] Buckley-Johnstone L, Harmon M, Lewis R, Hardwick C, Stock R. A comparison of friction modifier performance using two laboratory test scales. Proc Inst Mech Eng Part F J Rail Rapid Transit 2019;233:201–10. https://doi.org/10.1177/0954409718787045.

[48] Voltr P, Lata M. Transient wheel-rail adhesion characteristics under the cleaning effect of sliding. Veh Syst Dyn 2015;53:605–18. https://doi.org/10.1080/00423114.2014.961488.

[49] Omasta M, Navrátil V, Gabriel T, Galas R, Klapka M. Design and Development of a Twin Disc Test Rig for the Study of Squeal Noise from the Wheel – Rail Interface. Appl Eng Lett J Eng Appl Sci 2022;7:10–6. https://doi.org/10.18485/aeletters.2022.7.1.2.

[50] Matsumoto A, Sato Y, Ohno H, Mizuma T, Suda Y, Tanimoto M, et al. Study on curving performance of railway bogies by using full-scale stand test. Veh Syst Dyn 2006;44:862–73. https://doi.org/10.1080/00423110600907402.

[51] Zhang W, Chen J, Wu X, Jin X. Wheel/rail adhesion and analysis by using full scale roller rig. Wear 2002;253:82–8. https://doi.org/10.1016/S0043-1648(02)00086-8.

[52] Suzumura J, Sone Y, Ishizaki A, Yamashita D, Nakajima Y, Ishida M. In situ X-ray analytical study on the alteration process of iron oxide layers at the railhead surface while under railway traffic. Wear 2011;271:47–53. https://doi.org/10.1016/j.wear.2010.10.054.

[53] White BT, Lewis R, Olofsson U, Lyu Y. The Contribution of Iron Oxides to the Wet-Rail Phenomenon. Civil-Comp Proc., vol. 110, 2016. https://doi.org/10.4203/ccp.110.154.

[54] Zhu Y, Olofsson U, Chen H. Friction Between Wheel and Rail: A Pin-On-Disc Study of Environmental Conditions and Iron Oxides. Tribol Lett 2013;52:327–39. https://doi.org/10.1007/s11249-013-0220-0.

[55] Zhu Y, Lyu Y, Olofsson U. Mapping the friction between railway wheels and rails focusing on environmental conditions. Wear 2015;324–325:122–8. https://doi.org/10.1016/j.wear.2014.12.028.

[56] Galas R, Omasta M, Shi L, Ding H, Wang W, Krupka I, et al. The low adhesion problem: The effect of environmental conditions on adhesion in rolling-sliding contact. Tribol Int 2020;151:106521. https://doi.org/10.1016/j.triboint.2020.106521.

[57] Tomeoka M, Kabe N, Tanimoto M, Miyauchi E, Nakata M. Friction control between wheel and rail by means of on-board lubrication. Wear 2002;253:124–9. https://doi.org/10.1016/S0043-1648(02)00091-1.

[58] Ishida M, Ban T, Iida K, Ishida H, Aoki F. Effect of moderating friction of wheel/rail

interface on vehicle/track dynamic behaviour. Wear 2008;265:1497–503. https://doi.org/10.1016/j.wear.2008.02.041.

[59] Hardwick C, Lewis S, Lewis R. The effect of friction modifiers on wheel/rail isolation at low axle loads. Proc Inst Mech Eng Part F J Rail Rapid Transit 2014;228:768–83. https://doi.org/10.1177/0954409713488102.

[60] Sone Y, Suzumura J, Koga H, Tamoto Y, Ishida M, Yamazaki H, et al. Effects on braking distance from the use of traction fluid as a wheel/rail lubricant. Proc Inst Mech Eng Part F J Rail Rapid Transit 2015;229:89–96. https://doi.org/10.1177/0954409713502954.

[61] Hardwick C, Lewis R, Stock R. The effects of friction management materials on rail with pre existing rcf surface damage. Wear 2017;384–385:50–60. https://doi.org/10.1016/j.wear.2017.04.016.

[62] Messaadi M, Oomen M, Kumar A. Friction modifiers effects on tribological behaviour of bainitic rail steels. Tribol Int 2019;140. https://doi.org/10.1016/j.triboint.2019.105857.

[63] CEN/TS 15427–2-2:2021. Railway applications - Wheel/Rail friction management - Part 2–2: Properties and Characteristics - Top of Rail materials, 2021.

[64] Rahmani H, Gutsulyak D, Stanlake L, Stoeber B, Green S. Carrydown of liquid friction modifier. Proc Inst Mech Eng Part F J Rail Rapid Transit 2022;236:1124–34. https://doi.org/10.1177/09544097221076258.

[65] Lee ZS, Trummer G, Six K, Lewis R. Wheel/Rail Creep Force Model for Wayside Application of Top-of-Rail Products Incorporating Carry-On and Consumption Effects. Lect. Notes Mech. Eng., vol. 1, 2020, p. 669–77. https://doi.org/10.1007/978-3-030-38077-9_78.

[66] Lee ZS, Trummer G, Harmon M, White B, Six K, Lewis R. Studying the transfer mechanisms of water based top-of-rail products in a wheel/rail interaction. Proc Inst Mech Eng Part F J Rail Rapid Transit 2024;238:164–74. https://doi.org/10.1177/09544097231187679.

[67] Trummer G, Lee ZS, Lewis R, Six K. Modelling of Frictional Conditions in the Wheel–Rail Interface Due to Application of Top-of-Rail Products. Lubricants 2021;9:100. https://doi.org/10.3390/lubricants9100100.

[68] Kvarda D, Galas R, Omasta M, Hartl M, Krupka I, Dzimko M. Shear properties of top-of-rail products in numerical modelling. Proc Inst Mech Eng Part F J Rail Rapid Transit 2022. https://doi.org/10.1177/09544097221138374.

[69] Wu B, Shi L, Li J, Ding H, Galas R, Omasta M, et al. Rheological and tribological performance of top-of-rail friction modifiers with different viscosities. Wear 2024;538–539:205229. https://doi.org/10.1016/j.wear.2023.205229.

[70] Kvarda D, Skurka S, Galas R, Omasta M, Shi L, Ding H, et al. The effect of top of rail lubricant composition on adhesion and rheological behaviour. Eng Sci Technol an Int J 2022;35:101100. https://doi.org/10.1016/j.jestch.2022.101100.

[71] Vélez JC, Cornelio JAC, Sierra RB, Santa JF, Hoyos-Palacio LM, Nevshupa R, et al. Development of a composite friction modifier with carbon nanotubes for applications at the wheel–rail interface. Adv Compos Lett 2020;29:2633366X2093001. https://doi.org/10.1177/2633366X20930019.

[72] Zhu Y, Olofsson U, Persson K. Investigation of factors influencing wheel–rail adhesion using a mini-traction machine. Wear 2012;292–293:218–31. https://doi.org/10.1016/j.wear.2012.05.006.

[73] Oldknow K, Eadie DT, Stock R. The influence of precipitation and friction control agents on forces at the wheel/rail interface in heavy haul railways. Proc Inst Mech Eng Part F J Rail Rapid Transit 2013;227:86–93. https://doi.org/10.1177/0954409712452240.

[74] Matsumoto K, Suda Y, Fujii T, Komine H, Tomeoka M, Satoh Y, et al. The optimum design of an onboard friction control system between wheel and rail in a railway system for improved curving negotiation. Veh Syst Dyn 2006;44:531–40. https://doi.org/10.1080/00423110600875294.

[75] Khan SA, Lundberg J, Stenstrom C, Stenström C. Carry distance of top-of-rail friction modifiers. Proc Inst Mech Eng Part F-Journal Rail Rapid Transit 2018;232:2418–30. https://doi.org/10.1177/0954409718772981.

[76] Curley D, Anderson DC, Jiang J, Hanson D. Field Trials of Gauge Face Lubrication and Top-of-Rail Friction Modification for Curve Noise Mitigation. In: Nielsen JCO, Anderson D, Gautier PE, Iida M, Nelson JT, Thompson D, et al., editors. Noise Vib. Mitig. Rail Transp. Syst., vol. 126, 2015, p. 449–56. https://doi.org/10.1007/978-3-662-44832-8_54.

[77] Lewis SR, Lewis R, Olofsson U. An alternative method for the assessment of railhead traction. Wear 2011;271:62–70. https://doi.org/10.1016/j.wear.2010.10.035.

[78] Harmon M, Santa JF, Jaramillo JA, Toro A, Beagles A, Lewis R. Evaluation of the coefficient of friction of rail in the field and laboratory using several devices. Tribol - Mater Surfaces Interfaces 2020;14:119–29. https://doi.org/10.1080/17515831.2020.1712111.

[79] Folorunso MO, Lewis R, Lanigan JL. Effects of temperature and humidity on railhead friction levels. Proc Inst Mech Eng Part F J Rail Rapid Transit 2023;237:1009–24. https://doi.org/10.1177/09544097221148236.

[80] Khan SA, Lundberg J, Stenström C. The effect of third bodies on wear and friction at the wheel-rail interface. Proc Inst Mech Eng Part F J Rail Rapid Transit 2022;236:662–71. https://doi.org/10.1177/09544097211034688.

[81] Harrison H, McCanney T, Cotter J. Recent developments in coefficient of friction measurements at the rail/wheel interface. Wear 2002;253:114–23. https://doi.org/10.1016/S0043-1648(02)00090-X.

[82] Areiza YA, Garcés SI, Santa JF, Vargas G, Toro A. Field measurement of coefficient of friction in rails using a hand-pushed tribometer. Tribol Int 2015;82:274–9. https://doi.org/10.1016/j.triboint.2014.08.009.

[83] Harrison H. Development of a Third Generation Tribometer. CM2015-0130 2015;September.

[84] Spiryagin M, Persson I, Hayman M, Wu Q, Sun YQ, Nielsen D, et al. Friction measurement and creep force modelling methodology for locomotive track damage studies. Wear 2019;432–433:202932. https://doi.org/10.1016/j.wear.2019.202932.

[85] Persson I, Spiryagin M, Casanueva C. Influence of non-dry condition creep curves in switch negotiation. Veh Syst Dyn 2023;61:892–904.

https://doi.org/10.1080/00423114.2022.2037668.

[86] Eadie DT, Harrison H, Kempka R, Lewis R, Keylin A, Wilson N. Field assessment of friction and creepage with a new tribometer. Proc. 11th Int. Conf. Contact Mech. Wear Rail/wheel Syst. C. 2018, vol. 17, 2018, p. 208–17.

[87] Harrison H. The development of a low creep regime, hand-operated tribometer. Wear 2008;265:1526–31. https://doi.org/10.1016/j.wear.2008.03.028.

[88] Harrison H. Producing and measuring the 3rd body layer. 2020 Jt. Rail Conf., American Society of Mechanical Engineers; 2020, p. 1–7. https://doi.org/10.1115/JRC2020-8095.

[89] PCS Instruments -. Mini traction machine n.d. https://pcs-instruments.com/product/mtm/.

[90] Bruker. 3D optical profilometer ContourX-1000 n.d. https://www.bruker.com/en/products-and-solutions/test-and-measurement/3d-optical-profilers/contourx-1000.html (accessed July 26, 2024).

[91] Chen H, Namura A, Ishida M, Nakahara T. Influence of axle load on wheel/rail adhesion under wet conditions in consideration of running speed and surface roughness. Wear 2016;366–367:303–9. https://doi.org/10.1016/j.wear.2016.05.012.

LIST OF FIGURES AND TABLES

List of Figures

List of Tables

LIST OF SYMBOLS AND ABBREVIATIONS

CoT	(1)	Coefficient of traction
$creep$	(1)	Creep
D	(m)	Diameter of measuring wheel
I	(kg·m2)	Momentum of inertia
M_B	(Nm)	Braking torque
Q	(N)	Wheel load
r	(mm)	Radii
T	(N)	Traction force
v	(m/s)	Velocity
v_L	(m/s)	Longitudinal speed of measuring module
v_R	(m/s)	Tangential speed of measuring wheel
α	(rad/s2)	Angular acceleration
ω	(rad/s)	Angular velocity

AH	Absolute humidity
AoA	Angle of attack
BUT	Brno University of Technology
CoA	Coefficient of adhesion
CoF	Coefficient of friction
CoT	Coefficient of traction
CoT_e	Effective cot
FFT	Fast furrier transformation
FM	Friction modifier
HO	Hand-Operated
L/V	Lateral/Vertical
MTM	Mini traction machine
OLF	Over-lubrication factor
Q1 – Q4	Performance classes
RCF	Rolling contact fatigue
RH	Relative humidity
RTRI	Railway Technical Research Institute
SPL	Sound pressure level
SRR	Slip-to-rail ratio
TOR	Top-of-rail
TORL	Top-of-rail lubricant
TORP	Top-of-rail products
VHPF	Very high positive friction